Pharmacological Research 221 (2025) 107944

Contents lists available at ScienceDirect

Pharmacological Research

journal homepage: www.elsevier.com/locate/yphrs

Extracellular RNA drives TNF-α/TNF-receptor-1 mediated cardiac ischemia/reperfusion injury: Mechanistic insights and therapeutic potential of RNase1

Hector A. Cabrera-Fuentes [a,b,c,d,*], Marisol Ruiz-Meana [e], Guillermo Barreto [f], Victor L. Serebruany [g,h], Jose T. Sánchez-Vega [i], Eduardo Pérez-Campos [c,j], Sawa Kostin [k], Andreas Böning [l], Efrén Emmanuel Jarquín González [m], Ebtesam A. Al-Suhaimi [n], Julian Rodriguez-Montesinos [o], Javier Inserte [e], Sarah Pedretti [p], Jonathan Yap [q], Jason Irei [q], Daniel G. Sedding [r], Sandrine Lecour [p], Elisa A. Liehn [s,t], David Garcia-Dorado [e], Derek J. Hausenloy [s,u,v,w], William A. Boisvert [q,1], Klaus T. Preissner [x,**,1]

[a] División de Estudios de Posgrado e Investigación, Tecnológico Nacional de México / Instituto Tecnológico de Tijuana, Tijuana, BC 22414, Mexico
[b] R&D group, Vice Presidency Scientific Research & Innovation, Imam Abdulrahman bin Faisal University (IAU), P.O. Box 1982, Dammam 31441, Saudi Arabia
[c] UNAM-UABJO Research Centre, Faculty of Medicine and Surgery, Universidad Autónoma Benito Juárez de Oaxaca (UABJO), Oaxaca 68120, Mexico
[d] Dirección de la División de Investigación y Desarrollo Científico, Benemérita Universidad de Oaxaca, Oaxaca 68000, Mexico
[e] Cardiovascular Diseases Research Group, Vall d'Hebron Institut de Recerca (VHIR), Campus Vall d'Hebron Hospital, Barcelona & Centro de Investigacion Biomédica en Red de Enfermedades Cardiovasculares (CIBER-CV), Madrid, Spain
[f] Université de Lorraine, CNRS, Laboratoire IMoPA, UMR 7365, Nancy F-54000, France
[g] Department of Neurology, Johns Hopkins University School of Medicine, Baltimore, MD 21205, USA
[h] HeartDrug Research LLC, West Friendship, MD 21294, USA
[i] Parasitology Laboratory, Department of Microbiology and Parasitology, Faculty of Medicine, Universidad Nacional Autónoma de Mexico (UNAM), Mexico City, Mexico
[j] División de Estudios de Posgrado e Investigación, Tecnológico Nacional de México / Instituto Tecnológico de Oaxaca, Oaxaca 68030, Mexico
[k] Faculty of Health Sciences Brandenburg, Brandenburg Medical School Theodor Fontane, Neuruppin, Germany
[l] Department of Cardiovascular Surgery, Medical School, Justus-Liebig-University, Giessen, Germany
[m] Dirección General de los Servicios de Salud de Oaxaca, Secretaría de Salud, Servicios de Salud de Oaxaca, Oaxaca 68000, Mexico
[n] Vice Presidency for Scientific Research and Innovation, Imam Abdulrahman Bin Faisal University, Dammam, Saudi Arabia, P.O. Box 1982, Dammam 31441, Saudi Arabia
[o] Evotec International GmbH, Mangred Eigen Campus, Göttingen, Germany
[p] Cape Heart Institute, University of Cape Town, Cape Town, South Africa
[q] Center for Cardiovascular Research, John A. Burns School of Medicine, University of Hawaii, HI, USA
[r] Mid-German Heart Center, Division of Cardiology, Angiology and Intensive Medical Care, University Hospital Halle, Martin-Luther-University Halle-Wittenberg, Halle (Saale), Germany
[s] National Heart Research Institute Singapore, National Heart Center Singapore, Singapore, 5 Hospital Dr, Singapore 169609, Singapore
[t] Centre for Innovation and eHealth, University of Medicine and Pharmacy Carol Davila, Pitar Moș 20, Bucharest 030167, Romania
[u] Cardiovascular & Metabolic Disorders Program, Duke-National University of Singapore Medical School, Singapore
[v] Yong Loo Lin School of Medicine, National University Singapore, Singapore
[w] The Hatter Cardiovascular Institute, University College London, London, UK
[x] Kerckhoff-Heart Research Institute, Department of Cardiology, Medical School, Justus-Liebig-University, Giessen, Germany

ARTICLE INFO

Keywords:
Extracellular ribonucleic acid (eRNA)
Ribonuclease-1 (RNase1)

ABSTRACT

Myocardial ischemia/reperfusion (I/R) injury causes cardiomyocyte death and exacerbates inflammation. Emerging evidence implicates extracellular RNA (eRNA) and tumor necrosis factor-α (TNF-α) as key mediators.

* Correspondence to: Tecnológico Nacional de México / Instituto Tecnológico de Tijuana, División de Estudios de Posgrado e Investigación, Calz del Tecnológico 12950, Tomas Aquino, 22414 Tijuana, B.C, México.
** Correspondence to: Kerckhoff Heart Research Institute (KHFI) Medical Faculty, Justus Liebig University, Giessen 35392, Germany.
E-mail addresses: hafuentes@iau.edu.sa, hector.cf@tectijuana.edu.mx (H.A. Cabrera-Fuentes), klaus.t.preissner@biochemie.med.uni-giessen.de (K.T. Preissner).
[1] These two authors are joint senior authors

https://doi.org/10.1016/j.phrs.2025.107944
Received 31 July 2025; Received in revised form 25 August 2025; Accepted 6 September 2025
Available online 12 September 2025

Inflammation
Ischemia/reperfusion (I/R) injury
Acute myocardial infarction
Tumor necrosis factor-α (TNF-α)
TNF-α -converting-enzyme (TACE/ADAM17)
TAPI (TACE-Inhibitor)
Cardioprotection
Cell death mechanisms
Acute ST-segment elevation myocardial infarction (STEMI)
Creatine Kinase (CK)
Combination Therapy
Cyclosporine-A (CsA)
Mitochondrial permeability transition pore (mPTP)
Percutaneous coronary intervention (PCI)

We hypothesize that eRNA released from ischemic cardiomyocytes amplifies I/R injury via TNF-α/TNF-receptor-1 (TNF-R1) signaling, and that hydrolysis of eRNA by RNase1 can attenuate I/R injury by disrupting this pathway. Here, we investigated the mechanistic role of eRNA and its interplay with TNF-α signaling in cardiac I/R injury, and evaluated the therapeutic potential of RNase1 and cyclosporine-A (CsA). In ST-segment elevation myocardial infarction patients, plasma eRNA levels were significantly elevated 2 h post-percutaneous coronary intervention (PCI), correlating positively with Creatine Kinase (CK). In murine I/R and hypoxia/reoxygenation models, eRNA released from stressed cardiomyocytes acted as a damage-associated molecular pattern, triggering TNF-α shedding via TACE/ADAM17 and activating TNF-R1-mediated inflammation, mPTP opening, and cell death. Genetic deletion of TNF-α or TNF-R1 abrogated eRNA-induced cytotoxicity, while TNF-receptor- 2 (TNF-R2) deficiency exacerbated injury. Pharmacological inhibition of TACE with TAPI suppressed TNF-α release and preserved cell viability. RNase1 effectively degraded eRNA, blocking upstream pro-inflammatory signaling, whereas CsA preserved mitochondrial integrity by preventing mPTP opening. Notably, RNase1 and CsA showed synergistic protection *in vivo* when administered at reperfusion, significantly reducing myocardial infarct size. These findings identify eRNA as both a biomarker and pathogenic mediator of myocardial I/R injury, and support a dual-targeted strategy using RNase1 and CsA to interrupt the TNF-α/TNF-R1-driven inflammatory and mitochondrial death pathways. Targeting both upstream inflammatory and downstream mitochondrial mechanisms represents a promising cardioprotective intervention for acute myocardial infarction.

1. Introduction

Cardiomyocyte death during acute myocardial infarction significantly impacts the quality of life and survival of patients with coronary artery disease, one of the leading causes of morbidity and mortality in industrialized countries [1–4]. Following the rupture of atherosclerotic plaques and subsequent wound repair, coronary vessels often become occluded by thrombus material, leading to stenotic blood flow, reduced oxygen supply to the myocardium (ischemia), and oedema formation [5]. Although interventional coronary recanalization can reopen occluded arteries, it fails to prevent cell death occurring in the initial phase of reperfusion. This paradoxical phenomenon, known as "myocardial ischemia/reperfusion (I/R) injury," has been extensively studied in experimental animal models [6]. The mechanisms involved are intricate and multifaceted, involving Ca^{2+} overload [7], mitochondrial permeabilization through the opening of the mitochondrial permeability transition pore (mPTP) [8–10], ATP-dependent hyper--contraction [11,12], neutrophil infiltration and "Neutrophil extracellular traps" (NETs) formation [13], making it challenging to develop effective treatments. Additionally, the variability in individual responses and the difficulty in targeting specific pathways, without affecting others, further complicate the development of a cure. Thus, extensive experimental studies are performed on this phenomenon to gain a deeper understanding and identify potential therapeutic strategies [14].

Although preclinical studies have convincingly demonstrated that infarct size can be markedly reduced by interventions applied at the time of reperfusion [15], such as contractile blockers [16], inhibitors of Na^+/Ca^{2+} [17] or Na^+/H^+ exchange [18], exosomes derived from mesenchymal stromal cells (MSC-Exo) [13], acidified malonate [19,20], or particulate guanylate cyclase agonists [21,22], none of them have been successfully translated into clinical practice [23–25]. Experimental studies have largely overlooked the contribution of factors from irreversibly damaged cardiac tissue to I/R injury. Nevertheless, disrupted cells release cytosolic proteins such as Creatine Kinase (CK) and cardiac troponins during reperfusion, which serve as diagnostic markers [26–29].

Additionally, other intracellular components, including mitochondrial deoxyribonucleic acid (DNA) [30,31] and ribonucleic acids (RNA), denoted here as extracellular RNA (eRNA), are detectable in the extracellular space after several types of tissue damage, including hypoxia [32,33]. The majority of eRNA consists of ribosomal RNA [34–36], which binds to various basic proteins in blood plasma or on cell surfaces, thereby promoting numerous extracellular functions, particularly in the context of vascular diseases [37–39]. These functions include the activation of blood coagulation/thrombosis, the release of tumor necrosis factor (TNF)-α and other cytokines, and the promotion of inflammatory processes, including macrophage polarization and vasculogenesis/angiogenesis [40–42]. Thus, besides its function as a "Danger--associated molecular pattern" (DAMP) signal, eRNA acts as a potent cofactor in cardiovascular inflammation and thrombosis, especially under tissue-damaging or pathological conditions [43,44].

Recently, we demonstrated an essential role for eRNA and TNF-α as early alarm signals in cardiac tissue damage that determine the cell-destructive outcomes during cardiac I/R. TNF-α converting enzyme (TACE/ADAM17), a member of the ADAM (a disintegrin and metalloprotease domain) family of proteinases, regulates inflammatory processes by cleaving transmembrane proteins like TNF-α and its receptors, and is implicated in various inflammatory diseases [45,46]. Our previous work demonstrated that administering ribonuclease 1 (RNase1) or TAPI, an inhibitor of TACE, at the onset of ischemia successfully reduced pathological parameters characteristic of I/R injury and significantly improved early post-ischemic functional myocardial recovery [35].

Therefore, we hypothesized that eRNA, released from ischemic cardiomyocytes, amplifies myocardial I/R injury by inducing TNF-α shedding via TACE/ADAM17, thereby activating TNFR1-dependent inflammatory and mitochondrial death signaling. We further hypothesized that therapeutic hydrolysis of eRNA by RNase1, administered at the onset of reperfusion, would attenuate myocardial injury by disrupting the upstream eRNA–TACE/ADAM17–TNF-α/TNFR1 inflammatory axis. Moreover, in combination with CsA, RNase1 would provide synergistic cardioprotection by simultaneously targeting upstream inflammatory and downstream mitochondrial pathways.

In the current study, using *in vitro*, *ex vivo*, and *in vivo* models of cardiac I/R injury, we uncover a novel mechanistic link between eRNA and TNF-α-receptor-mediated signaling pathways contributing to mitochondrial failure and cardiomyocyte death. Our findings highlight mitochondria as a downstream target of eRNA/TNF-α signaling, supporting a combined therapeutic approach as a novel cardioprotective strategy in the context of ischemic heart disease.

2. Results

2.1. eRNA levels positively correlate with CK_{max} serum concentration in STEMI patients

To identify the eRNA changes secondary to cardiac I/R injury, two groups of patients were studied: (a) eleven matched-control patients (63 % males, mean age 75 ± 5 years) and (b) twelve ST-segment elevation myocardial infarction (STEMI) patients (67 % males, mean age 75 ± 6 years). The groups did not differ in age (difference −0.16 years, 95 % confidence interval [CI] −4.70 to 4.38; p = 0.9422, unpaired two-tailed t-test) **(**Fig. 1**A)**. As shown in Fig. 1**B**, plasma eRNA levels were significantly higher 2 h post-percutaneous coronary intervention (PCI)

in STEMI patients compared to control-matched patients (595 ± 150 *vs.* 273 ± 38 ng/ml; p = 0.0004; 95 % CI 219–427 ng/ml; p = 0.0004, Welch's t-test). Likewise, peak serum CK levels (CK_{max}) were markedly elevated in STEMI patients compared with control subjects, showing an over 20-fold increase at 2 h post-PCI (2248 ± 1023 vs. 91 ± 30 U/L; 95 % CI 1507–2807 U/L; p < 0.0001, Welch's t-test) **(**Fig. 1**C).** Across all participants (n = 23), plasma eRNA levels were strongly correlated with CK_{max} (r = 0.9383; 95 % CI 0.86–0.97; P < 0.0001, Pearson's correlation) (Fig. 1**D**), indicating that higher eRNA levels were associated with larger infarct size.

2.2. Hypoxia-induced eRNA release enhances I/R injury

To elucidate the mechanisms of action of eRNA-induced cardiac injury, we first quantified eRNA released from cardiomyocytes exposed to hypoxia or normoxia. In murine cardiomyocytes exposed to 1 h hypoxia, the concentration of eRNA detected in the supernatant was significantly higher than the eRNA detected at 3 h of normoxia (155 ± 23 ng/mg protein *vs.* 72 ± 11 ng/mg protein, respectively; p = 0.0019) (Fig. 2**A**). The addition of TNF-α significantly enhanced the release of eRNA by at least 1.5-fold, both under normoxic (Control 72 ± 11 *vs.* TNF-α 140 ± 12 ng/mg protein; p = 0.0061) and hypoxic conditions (Control 155 ± 23 *vs.* TNF-α 212 ± 19; ng/mg protein; p = 0.016) (Fig. 2**A**). Exposure of cardiomyocytes to eRNA led to a significant sensitization of cardiomyocytes towards mPTP opening (Fig. 2**B**) as detected by the time at which sudden decrease of mitochondrial tetramethyl-rhodamine-ethylester (TMRE) occurred in response to oxidative stress (laser illumination). Such decay in mitochondrial fluorescence is followed by an abrupt increase in the cytosolic fluorescence due to the redistribution of TMRE and the occurrence of

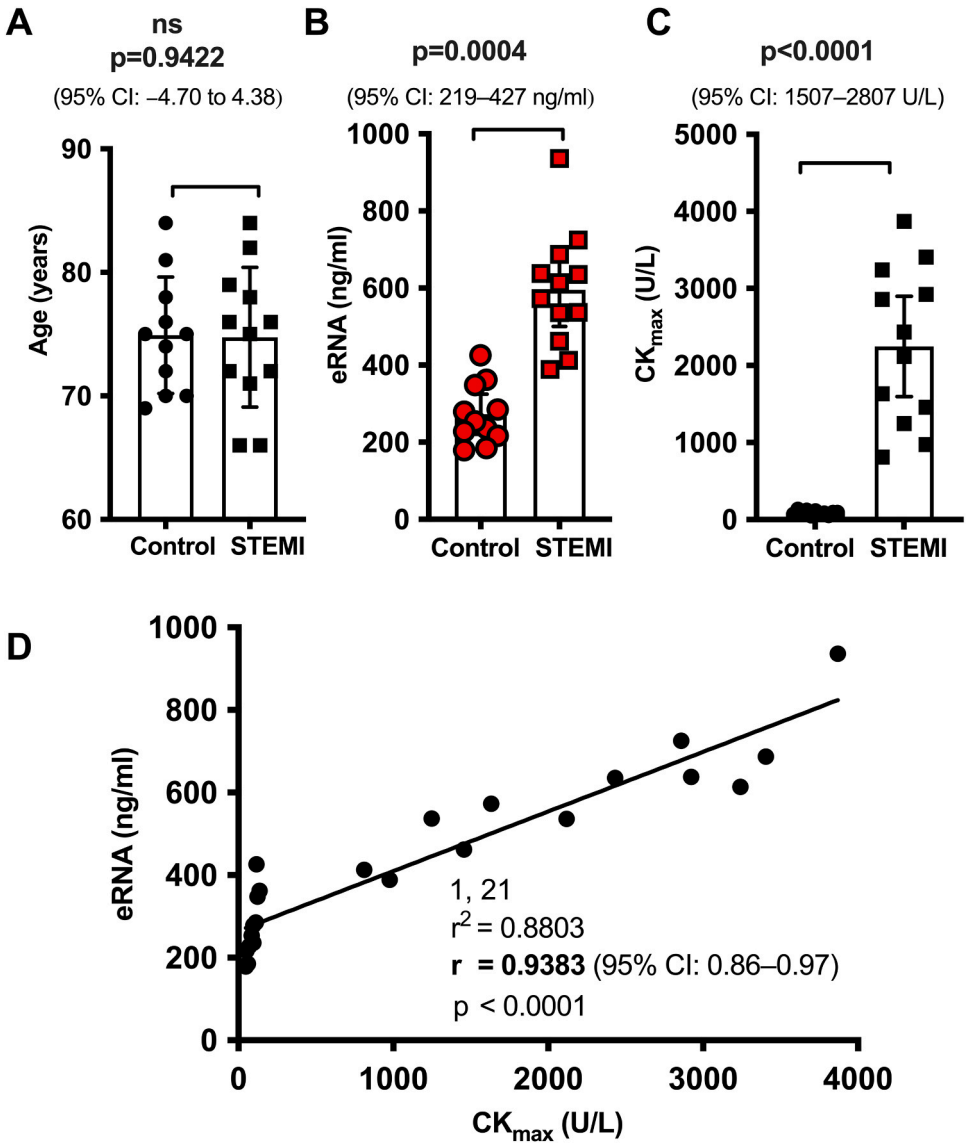

Fig. 1. Association between circulating eRNA and serum creatinine kinase (CK) in matched-control and in STEMI-patients. (A) Age of participants in matched-control (n = 11) and STEMI patients (n = 12) 2 h post-percutaneous coronary intervention (PCI). No significant difference was observed (74.9 ± 4.7 vs. 74.8 ± 5.7 years; difference −0.16 years, 95 % CI: −4.70 to 4.38; p = 0.9422, unpaired two-tailed *t*-test). (B) Plasma eRNA concentrations in both groups. Data are mean ± SD of triplicate measurements per individual. Levels were significantly elevated in STEMI patients compared with controls (595 ± 150 vs. 273 ± 38 ng/ml; 95 % CI: 219–427 ng/ml; p = 0.0004, Welch's *t*-test). (C) Peak serum creatine kinase levels (CK_{max}) in both groups. Data are mean ± SD of triplicate measurements per individual. CK_{max} was markedly higher in STEMI patients compared with controls (2248 ± 1023 vs. 91 ± 30 U/L; 95 % CI: 1507–2807; p < 0.0001, Welch's *t*-test). (D) Correlation between plasma eRNA and CK_{max} levels in all participants (n = 23) assessed using Pearson's correlation coefficient. A strong positive correlation was observed (r = 0.9383; 95 % CI: 0.86–0.97; p < 0.0001).

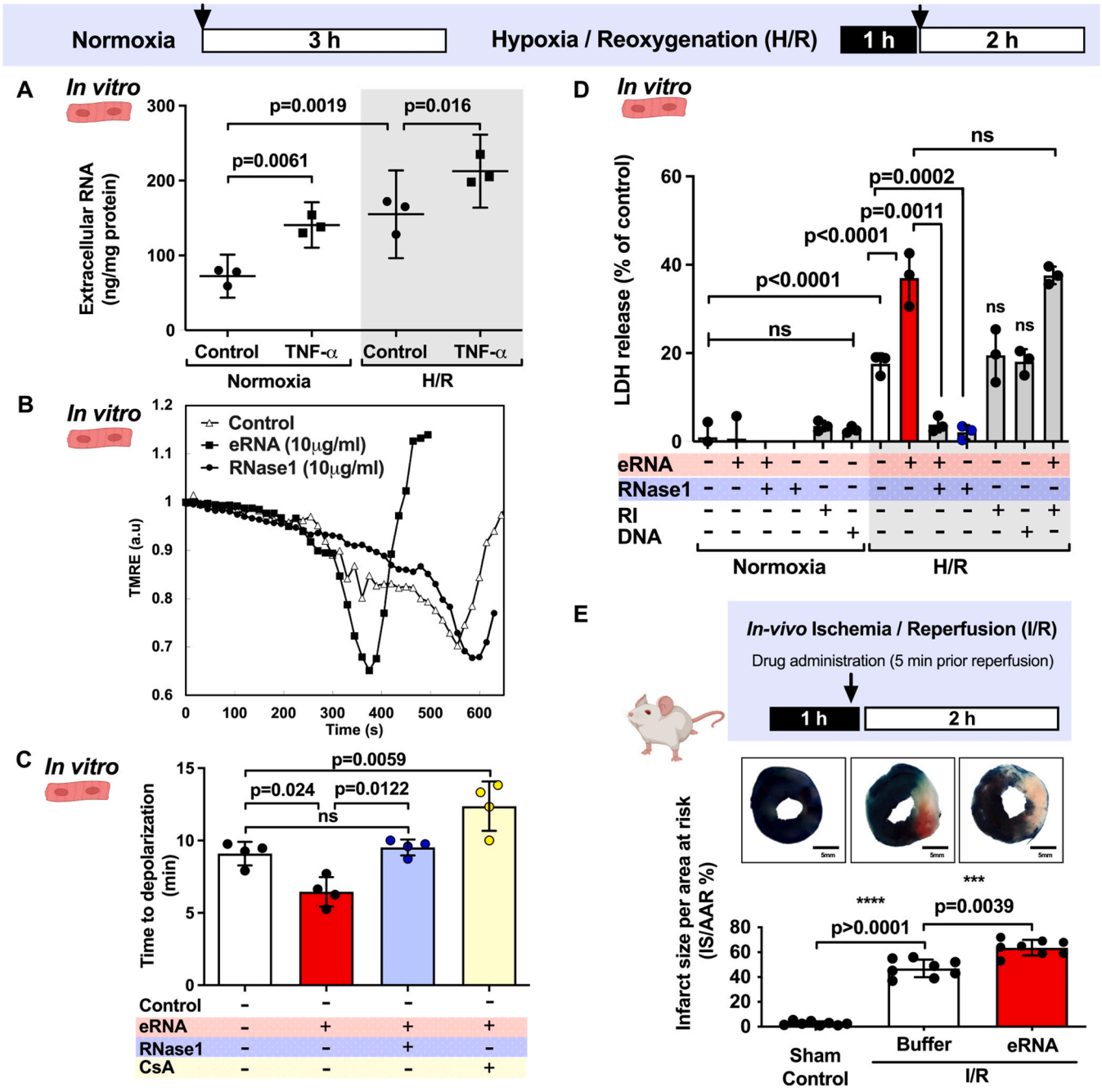

Fig. 2. eRNA enhances hypoxia-induced cell death. Experimental Scheme: Cardiomyocytes were incubated under normoxic conditions (21 % O_2) at 37°C for 3 h, with pharmacological treatments administered at the start of incubation. For hypoxia/reoxygenation (H/R) experiments, cardiomyocytes were exposed to 1 h of hypoxia followed by 2 h of reoxygenation at 37°C. Treatments were applied at the onset of reoxygenation without medium exchange to simulate reperfusion conditions. (A) Extracellular RNA (eRNA) was quantified under normoxia (3 h) or hypoxia (1 h) in supernatant of untreated (-) or TNF-α-treated cardiomyocytes. Values represent mean ± SD (n = 4 independent experiments per group). (B) Changes in the intensity of fluorescence, induced by intermittent laser illumination in TMRE-loaded cardiomyocytes, were registered under control conditions or in the presence of eRNA (10 μg/ml) or RNase1 (10 μg/ml). (C) Changes in the intensity of fluorescence induced by intermittent laser illumination in TMRE-loaded cardiomyocytes were registered and the time of maximal cell shortening, reflecting mPTP opening secondary to oxidative damage, was quantified in the absence (control) or presence of eRNA, RNase1 or cyclosporine-A (CsA, 1 μmol/L), respectively. Values represent mean ± SEM (n = 4 independent experiments per group) (D) Following treatment of cardiomyocytes with eRNA (10 μg/ml), hydrolyzed RNA (10 μg/ml), RNase1 (10 μg/ml), RNase-inhibitor (RI, 40 mU/ml) or DNA (10 μg/ml) under normoxia (3 h) or hypoxia (1 h) as indicated, the released lactate dehydrogenase (LDH) was quantified in each cell supernatant as an index of sarcolemmal rupture. Values represent mean ± SD (n = 4 independent experiments per group). (E) Following the induction of the *in vivo* acute cardiac I/R mice model, infarct size in mice hearts was quantified after coronary occlusion followed by 2 h reperfusion in the absence (Buffer solution) or presence of eRNA (15 μg/mouse). Buffer solution or eRNA was administrated intravenously (*i. v.*) 5 min before reperfusion. Representative pictures show myocardial infarct size in heart sections indicated by dual staining with 2,3,5-triphenyltetrazolium chloride (TTC) / Evans blue. Scale bar, 5 mm. Data represent mean ± SD (n = 8 mice per group). For all panels: *p < 0.05, **p < 0.01, ***p < 0.001, ns= not significant; or exact p-value shown. Statistical significance was determined by one-way ANOVA with Bonferroni's post hoc test or unpaired Student's *t*-test, as appropriate.

cell shortening (secondary to ATP depletion). Indeed, the time at which rigor contracture occurred was significantly shortened in cardiomyocytes exposed to eRNA (Control 9 ± 0.8 *vs.* RNA 6.4 ± 1 min; p = 0.024) (Fig. 2**C**). The addition of RNase1 abolished the sensitizing effect of eRNA (p = 0.0122) on mPTP opening, as reflected by a delay in the time necessary to induce rigor contracture to a value that was similar to that obtained in control cells (Control 9 ± 0.8 *vs.* RNase1 9.5 ± 0.5 min; p = 0.9464). Addition of CsA resulted in a similar delaying effect on mPTP-mediated cell contracture (CsA 12.4 ± 1.7 min; p = 0.0059), as previously reported [8,47] (Fig. 2**C**). Dysregulated mPTP opening uncouples oxidative phosphorylation eventually leading to energy collapse and cell death [7,48–50]. Under normoxia, addition

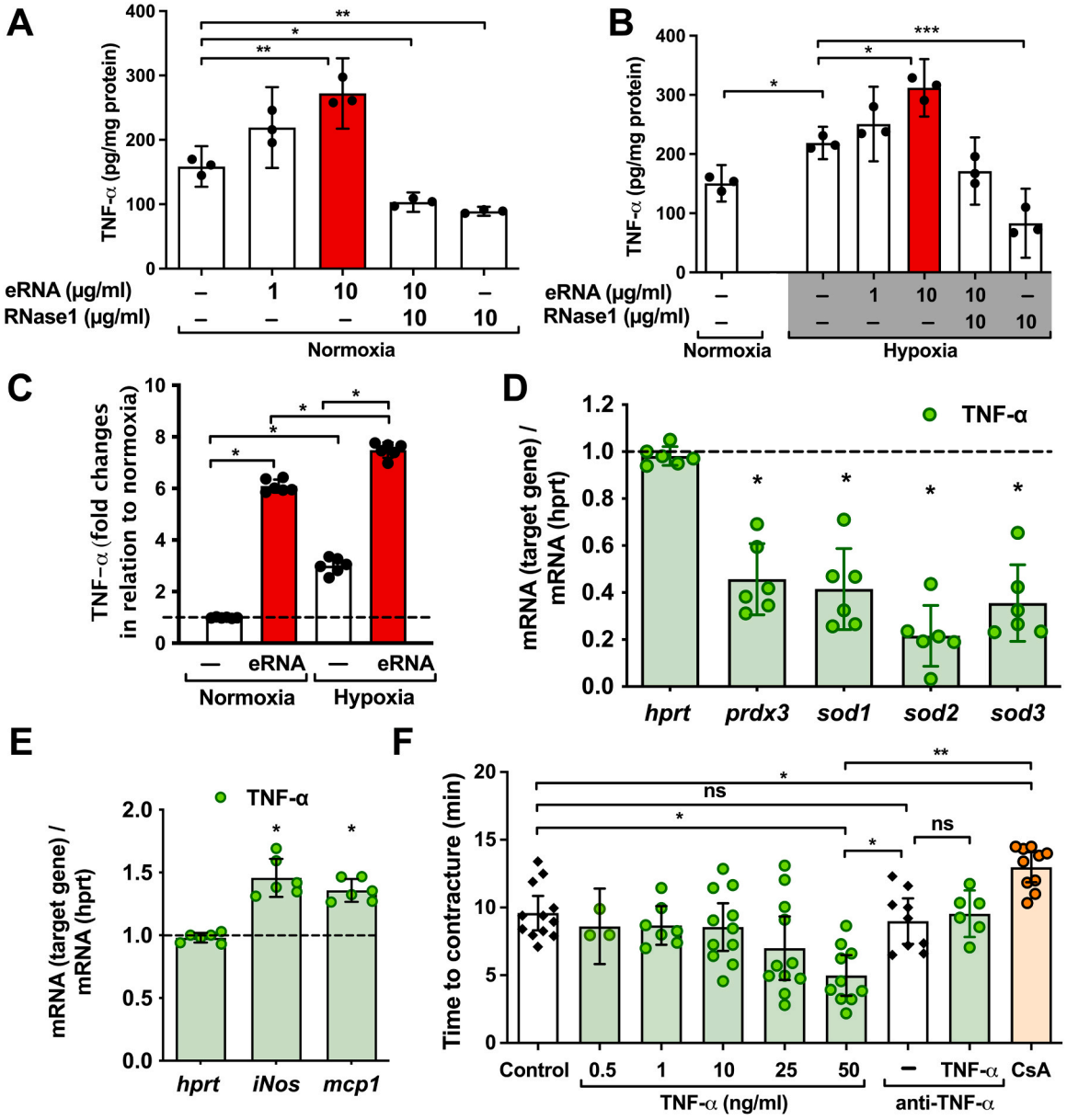

Fig. 3. Extracellular RNA potentiates the release of TNF-α from cardiomyocytes under hypoxia. (A) TNF-α was quantified in cardiomyocyte supernatants previously treated for 3 h under normoxia with eRNA (1 or 10 μg/ml), with hydrolyzed RNA or RNase1 (10 μg/ml), respectively. (B) Cardiomyocytes were treated under normoxia (3 h) or hypoxia (1 h) with eRNA, hydrolyzed RNA or RNase1 (10 μg/ml), respectively, followed by analysis of TNF-α in corresponding cell supernatants. Values represent mean ± SD (n = 3 independent experiments per group). (C) TNF-α levels were quantified by enzyme-linked immune- sorbent assay (ELISA), demonstrating a significant increase following eRNA treatment under normoxic and hypoxic conditions. (D) The mRNA level of peroxiredoxin-3 (Prdx3) and superoxide-dismutases (Sod) 1–3 in cardiomyocytes treated with TNF-α (20 ng/ml) for 3 h under normoxia, were quantified by quantitative real time PCR analysis (qRT-PCR), and compared to non-treated cells (control). Data represent changes in the ratio between target and hprt mRNA (n = 3 independent experiments per group, each in duplicate). (E) Changes in cellular mRNA levels of inducible NO-synthase (iNos) and monocyte chemotactic protein-1 (Mcp1) in cardiomyocytes, untreated (control) or treated with TNF-α (20 ng/ml) for 3 h under normoxia, were quantified by RT-PCR (n = 3 independent experiments per group, each in duplicate). (F) Following intermittent laser illumination, the time span at maximal cell shortening of cardiomyocytes secondary to mPTP opening was analysed in the absence (control) or presence of increasing concentrations of TNF-α in isolated TMRE-loaded cardiomyocytes. In a subset of experiments, anti-TNF-α (25 μg/ml; in the absence (-) or presence of TNF-α, 50 ng/ml) as well as CsA, 1 μmol/L were included. Data represent mean ± SEM of n > 20 cells per group. For all panels: *p < 0.05, **p < 0.01, ***p < 0.001, ns= not significant. Statistical significance was determined by one-way ANOVA with Bonferroni's post hoc test or unpaired Student's *t*-test, as appropriate.

of eRNA, RNase1, RNase inhibitor (RI) or DNA did not induce the LDH release in cardiomyocytes. By contrast, exposure to 1 h hypoxia followed by 2 h reoxygenation induced a substantial increase of LDH release, indicative of sarcolemmal rupture (Normoxia 0.96 ± 3 *vs.* Hypoxia 17.6 ± 2.3 %; $p < 0.0001$). Additional exposure to eRNA (37 ± 6 %; $p < 0.0001$), but not to hydrolyzed RNA, DNA or RI, resulted in a further elevation of LDH release that was almost completely prevented by treatment with RNase1 (2.1 ± 1.5 %; $p = 0.0002$), independent of the presence of exogenous eRNA (Hydrolyzed RNA 3.8 ± 1.7 %; $p = 0.0011$) (Fig. 2**D**). The cytotoxic effect of eRNA was further validated in an *in vivo* murine cardiac I/R injury model. In this model, infarct size (expressed as the percentage of the area of risk) was significantly larger in those hearts exposed to total cellular RNA (15 μg/mouse, obtained from freshly isolated cardiomyocytes) for 5 min prior to reperfusion with respect to control hearts (Control 47 ± 7 *vs.* RNA 64 ± 6 %; $p = 0.0039$). These results indicate the role of eRNA in exacerbating cardiac necrosis during I/R injury (Fig. 2**E**).

2.3. Hypoxia and eRNA promote cardiac I/R-induced TNF-α release

We have previously demonstrated that exposure of human monocytes to eRNA resulted in the induction of TNF-α release, which largely relied on the sheddase TNF-α-converting enzyme (TACE/ADAM17) [40,41]. Likewise, cardiomyocytes stimulated with eRNA (10 μg/ml) displayed a significant increase in TNF-α release (Control 159 ± 13 *vs.* RNA 272 ± 22 pg/mg protein; $p < 0.0001$) that could be effectively prevented by the addition of RNase1 (89 ± 3 pg/mg protein; $p = 0.0028$) (Fig. 3**A**). Importantly, incubation of cardiomyocytes with eRNA for 1 h under hypoxia led to a significantly elevated TNF-α release (312 ± 19 pg/mg protein; $p = 0.0004$) which was completely prevented by RNase1 treatment (83 ± 23 pg/mg protein; $p < 0.0001$) (Fig. 3**B**). Even under control conditions in which RNase1 kept the level of TNF-α at a minimum, eRNA induced a significant increase in TNF-α levels under both normoxic and hypoxic conditions, as confirmed by ELISA (Fig. 3**C**). Exposure of isolated cardiomyocytes to TNF-α for 3 h under normoxia significantly reduced mRNA levels of antioxidant enzymes such as peroxiredoxin-3 (*prdx3*) and all three isoforms of superoxide dismutase (*sod*), namely the cytoplasmic *sod1*, the mitochondrial *sod2* and the extracellular *sod3* (Fig. 3**D**). Also, TNF-α stimulation of cardiomyocytes markedly increased the expression of the pro-inflammatory cytokine mcp1 as well as *iNos* (Fig. 3**E**). Furthermore, TNF-α sensitized the cardiomyocytes towards mPTP opening and induced cardiomyocyte contracture in a dose-responsive manner, showing maximal significant effect at 50 ng/ml of TNF-α (Control 9.5 ± 3 *vs.* TNF-α 4.9 ± 2 min; $p = 0.0004$), whereas anti-TNF-α (8.9 ± 2 min; $p = 0.9996$) reversed this effect (Fig. 3**F**). As an established protective agent, CsA (12.97 ± 1.5 min; $p = 0.0242$) markedly prolonged the time to cardiomyocyte contracture.

2.4. Cytoprotective effects of TACE-inhibition

To elucidate the mechanism underlying eRNA-induced release of TNF-α, we investigated the role of the metalloproteinase TACE/ADAM17, a key sheddase responsible for converting membrane-bound pro-TNF-α into its soluble, active form [41]. In murine isolated cardiomyocytes, stimulation with eRNA (10 μg/ml) under normoxic conditions for 3 h significantly increased TNF-α release compared to controls (272.1 ± 22 *vs.* 167.2 ± 20.7 pg/mg protein; $p < 0.001$; Fig. 4**A**). eRNA-induced TNF-α release was significantly prevented in the presence of the metalloproteinase inhibitors GM6001 (10 μmol/L) or by the specific TACE inhibitor TAPI (10 μg/ml), which reduced TNF-α concentrations to 77.8 ± 8.7 1 pg/mg protein and 85.0 ± 6.9 1 pg/mg protein, respectively, in the presence of eRNA ($p < 0.001$ *vs.* eRNA alone). Likewise, both inhibitors significantly reduced baseline TNF-α levels when administered alone (GM6001: 86.5 ± 12.4 pg/mg protein; TAPI: 86.8 ± 14.1 pg/mg protein; $p < 0.001$ *vs.* control). Notably, no significant differences were observed between inhibitor-treated cardiomyocytes with or without eRNA stimulation, indicating effective suppression of eRNA-induced TNF-α release. Moreover, TNF-α levels did not differ significantly between GM6001 and TAPI, in either condition. These findings confirm a pivotal role for metalloproteinase activity in eRNA-induced TNF-α release. (Fig. 4**A**).

To further delineate the role of intracellular signaling, inhibition of NF-κB activation with the IκB phosphorylation inhibitor Bay11–7082 (10 μmol/L) significantly attenuated TNF-α release both when applied alone (66.5 ± 9.1 pg/mg protein; $p < 0.001$ *vs.* control) and in combination with eRNA (115.4 ± 9.9 pg/mg protein; $p < 0.0038$ *vs.* control), implicating canonical NF-κB signaling in the eRNA-induced response. However, TNF-α levels remained significantly higher with eRNA plus Bay11–7082 compared to Bay11–7082 alone ($p = 0.0071$), indicating a partial but meaningful contribution of NF-κB. These findings underscore the predominant role of metalloproteinases - particularly TACE - in mediating eRNA-induced TNF-α shedding. Finally, neutralization of TNF-α using a monoclonal antibody (25 μg/ml) fully suppressed cytokine levels, irrespective of eRNA exposure (14.3 ± 8.6 and 20.6 ± 4.9 pg/mg protein, respectively; $p < 0.0001$ *vs.* control), thereby confirming the specificity of the assay and the central role of TNF-α in this model (Fig. 4**A**).

The concentrations for GM6001, TAPI, Bay11, and anti–TNF-α were selected based on previous studies demonstrating that eRNA-induced TACE activation and TNF-α shedding are effectively inhibited *in vitro* under these conditions [51]. Moreover, under normoxic conditions (3 h), treatment with eRNA, TNF-α, or TAPI alone did not significantly increase LDH release in murine cardiomyocytes compared to control, indicating preserved sarcolemmal integrity. In contrast, exposure to H/R significantly increased LDH release (Normoxia: 16 ± 4 % *vs.* H/R: 40 ± 8 %; $p < 0.0001$), consistent with sarcolemmal disruption (Fig. 4**B**). Addition of exogenous TNF-α during reoxygenation further exacerbated cardiomyocyte injury (63.6 ± 5 %; $p < 0.0001$ *vs.* H/R), while TAPI treatment did not significantly alter LDH release compared to H/R alone (43.3 ± 6 %; $p > 0.99$). Co-administration of TNF-α and eRNA (66.6 ± 6 %) did not significantly amplify cytotoxicity beyond TNF-α alone, indicating a potential saturation of the TNF-α-induced cytotoxic response. Notably, TAPI significantly attenuated TNF-α-induced ($p = 0.0262$) and TNF-α + eRNA-induced ($p = 0.0037$) LDH release, but had no effect on hypoxia-induced injury alone ($p > 0.99$), in contrast to the protective profile observed with RNase1 **(**Fig. 2**D)**. These findings suggest that, while inhibition of TACE/TNF-α shedding confers significant protection, upstream targeting of eRNA with RNase1 offers superior cytoprotection by mitigating the initiating trigger of the TNF-α axis.

Furthermore, the effect of TAPI was investigated in the isolated perfused heart model exposed to I/R. TAPI was administered 30 min prior to the ischemic phase. TNF-α release (pre-ischemic values 12 ± 5 *vs.* maximal peak 85 ± 10 pg/min; $p = 0.0032$) was significantly reduced upon treatment with TAPI (22 ± 8 pg/min; $p = 0.0273$) (Fig. 4**C**). TAPI-treatment also decreased LDH release (Fig. 4**D**) in comparison to the untreated I/R group. The cumulative LDH release was also markedly reduced (I/R 143 ± 25 *vs.* I/R+TAPI 53 ± 13 UI/g tissue; $p = 0.0249$) along with a significant reduction in infarct size by 14 % (I/R 45 ± 7 *vs.* I/R+TAPI 31 ± 8 %, $p = 0.0249$) (Fig. 4**E**). Administration of TAPI preserved cardiac tissue architecture and prevented reperfusion-induced reactive oxygen species (ROS) burst from 211 ± 17 AU/μm^2 in I/R hearts to 91 ± 10 AU/μm^2 in TAPI treated group ($p < 0.0001$), as detected by confocal microscopy using a previously described approach [35] (Fig. 4**F-G**). These data indicate that the TACE-inhibitor TAPI exerts a similar protective role as that previously documented for RNase1 [34,35].

2.5. eRNA-induced cell death under hypoxic conditions requires TNF-receptor-1 activation

The role of TNF signaling in eRNA-induced cardiomyocyte death was

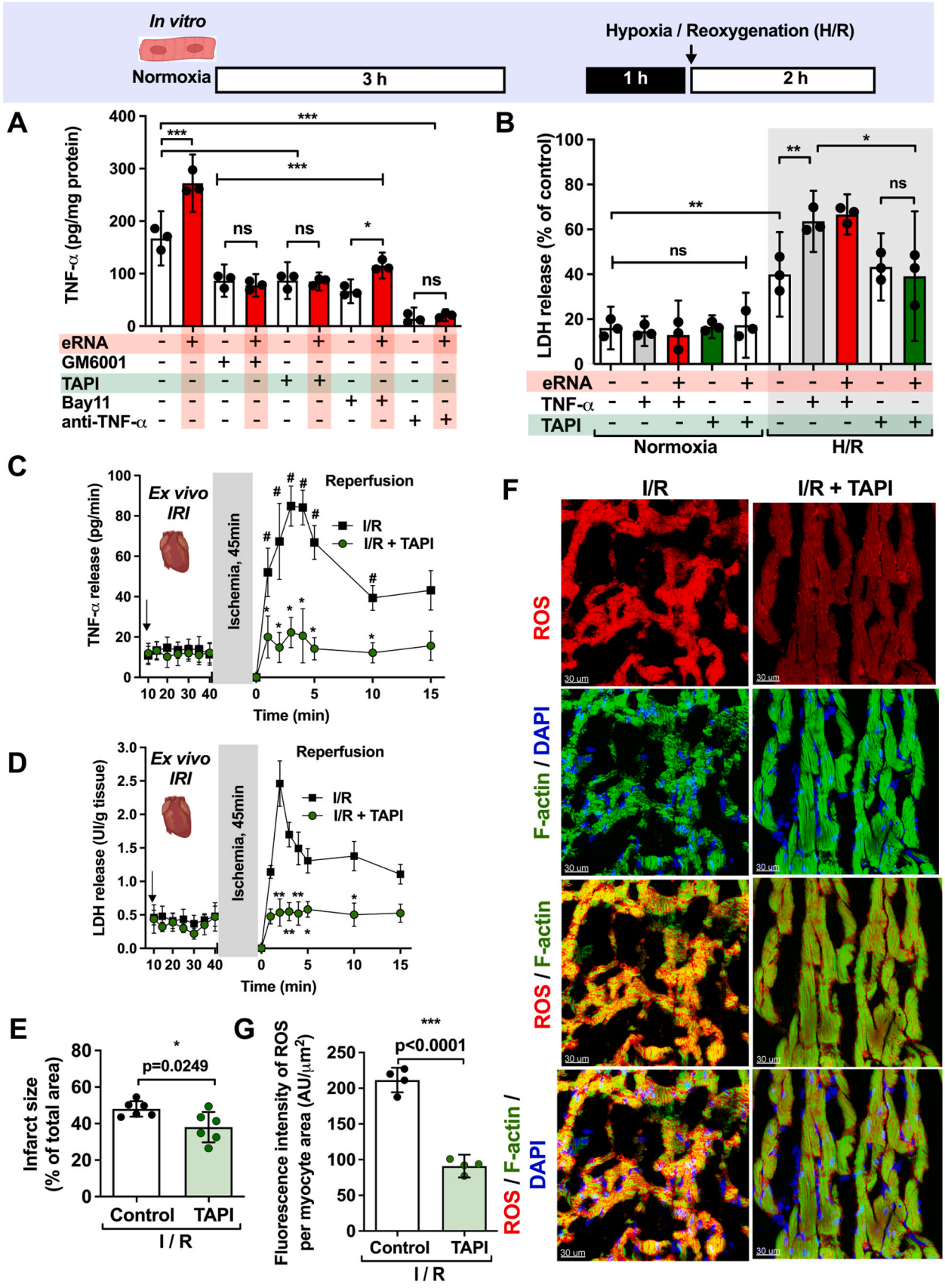

(caption on next page)

Fig. 4. Inhibition of metalloproteinases prevents TNF-α shedding and cell death. Experimental Scheme: Cardiomyocytes were incubated under normoxic conditions (21 % O_2) at 37°C for 3 h, with pharmacological treatments administered at the start of incubation. For hypoxia/reoxygenation (H/R) experiments, cardiomyocytes were exposed to 1 h of hypoxia followed by 2 h of reoxygenation at 37°C. Treatments were applied at the onset of reoxygenation without medium exchange to simulate reperfusion conditions. (A) Cardiomyocytes were treated for 3 h under normoxia in the absence (-) or presence of eRNA (10 μg/ml, grey zones) with GM6001 (10 μmol/L), TAPI (10 μg/ml), Bay11 (10 μmol/L) or anti-TNF-α (25 μg/ml) followed by quantification of TNF-α protein in the corresponding cell supernatants. Values represent mean ± SD (n = 3 independent experiments per group); *p < 0.05, ***p < 0.001; by one-way ANOVA followed by Bonferroni's test. (B) Following treatment of cardiomyocytes with eRNA (10 μg/ml) or TNF-α (20 ng/ml) in the absence (-) or presence of TAPI (10 μg/ml) under normoxia (3 h) or hypoxia (1 h, grey zone), the released LDH was quantified in the respective cell supernatants. Values represent mean ± SD (n = 3, independent experiments per group), *p < 0.05, **p < 0.01, ***p < 0.001, ns=non-significant; by one-way ANOVA followed by Bonferroni's test. (C) Isolated rat hearts (Langendorff-model) were submitted to I/R (45 min/120 min) in the absence (Buffer solution) or presence of TAPI (1 μmol/L). TAPI (1 μmol/L) was continuously administrated starting 30 min prior ischemic phase, for both set of experiments the stabilization phase was of 40 min. Release of TNF-α was quantified in the perfusate fractions throughout the 40 min stabilization and the first 15 min reperfusion period in Langendorff hearts submitted to I/R protocol alone or after administration (arrow) of TAPI (1 μmol/L). TNF-α values are corrected for respective flow rate and normalized to the effluent protein concentration; they represent mean ± SD (n = 3 hearts per group); $^{\#}$p < 0.001 (I/R *vs.* pre-ischemic values); *p < 0.001 (I/R+RNase1 *vs.* I/R) at the determined time points; statistical significance was assessed using Student's *t*-test for comparisons between two groups. (D) In Langendorff hearts submitted to I/R protocol alone or after administration (arrow) of TAPI (1 μmol/L), LDH release was quantified in the perfusate fractions throughout the 40-min stabilization and the first 15 min reperfusion period. LDH values are normalized to tissue weight and are expressed as mean ± SD (n = 3 hearts per group); *p < 0.05, **p < 0.01 *vs.* I/R at the determined time points; statistical significance was assessed using Student's *t*-test for comparisons between two groups. (E) Infarct size was quantified by the TTC reaction in heart sections and expressed as the percentage of necrotic tissue with respect to total ventricular mass in the different treatment groups indicated. Values represent mean ± SD (n = 6 hearts per group); p = 0.0249; by Student's t test. (F) Microslices obtained from the isolated Langendorff-perfused hearts submitted to 30 min stabilization followed by 45 min ischemia and 120 min reperfusion (I/R) alone or in the presence of TAPI (1 μmol/L) were analyzed by immunofluorescent staining. (G) Quantitative analysis of ROS (dihydroethidium) production described in (G) was performed; values represent mean ± SD (n = 3 hearts per group); p < 0.0001; by Student's t test. ROS (dihydroethidium, red) production together with detection of F-actin (green) and nuclear DNA (DAPI, blue) was analyzed by confocal microscopy. Representative images of multiple experiments are shown.

further investigated by quantifying LDH release as a marker of cell membrane damage. Primary cardiomyocytes were isolated from WT, TNF-α knockout (TNF-α-/-), TNF receptor 1-knockout (TNF-R1-/-), and TNF receptor 2 knockout (TNF-R2-/-) mice, and exposed to normoxic or H/R conditions in the presence or absence of eRNA. TNF-R1, known for its death domain, is primarily associated with pro-apoptotic and pro-inflammatory signaling, while TNF-R2 (lacking an intracellular death domain) generally promotes cell survival and tissue repair, highlighting the importance of their distinct roles crucial in the context of cardiomyocyte death and survival [52,53].

In WT cardiomyocytes, LDH release was minimal under normoxia (15.7 ± 4 % of control), increased significantly upon H/R (40.7 ± 13 % of control; p = 0.001 *vs.* normoxia), and was further elevated in the presence of eRNA (59.5 ± 8 % of control; p < 0.0001 *vs.* normoxia; p = 0.0096 vs H/R alone), indicating that eRNA exacerbates H/R-induced cell death in a statistically significant manner **(**Fig. 5**A).**

In TNF-α-/- cardiomyocytes, LDH release was also low under normoxia (24.4 ± 5 % of control) and significantly increased after H/R (43.2 ± 9 % of control; p = 0.0048 *vs.* normoxia). However, unlike WT cells, the addition of eRNA did not significantly enhance LDH release (43.2 ± 10 % of control *vs.* H/R; p > 0.9999), although it remained significantly higher than under normoxia (p = 0.0049), suggesting that TNF-α is necessary for the eRNA-mediated amplification of cell death **(**Fig. 5**B).** TNF-R1-/- cardiomyocytes showed low LDH levels under normoxia (23 ± 9 % of control), with a significant increase upon H/R (51.9 ± 11.2 % of control; p = 0.0024 *vs.* normoxia). Similar to TNF-α-/- cardiomyocytes, the addition of eRNA did not significantly enhance LDH release (48 ± 14.9 % of control *vs.* H/R; p > 0.99), although levels remained significantly higher than under normoxia (p = 0.0125) (Fig. 5**C**). In contrast, TNF-R2-/- cardiomyocytes exhibited a response

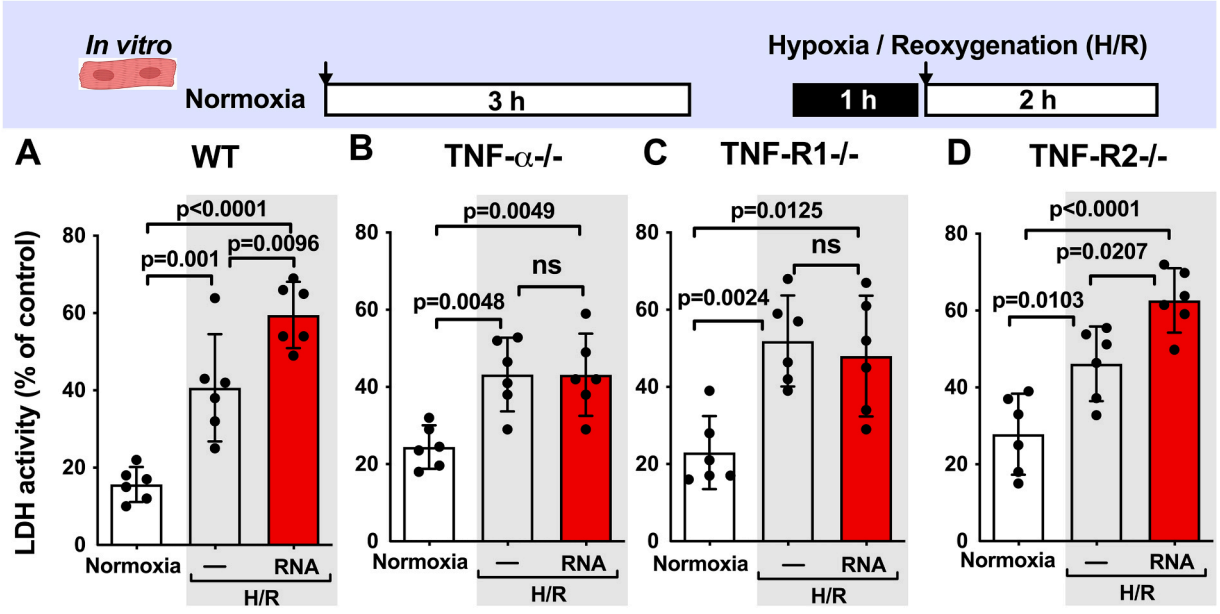

Fig. 5. TNF signaling is involved in eRNA-induced cell death. Release of LDH from cardiomyocytes was quantified in the supernatant from (A) wild-type (WT), (B) TNF-α-/- mice, (C) TNF-receptor-1 (TNF-R1)-/- mice, or (D) TNF-receptor-2 (TNF-R2)-/- mice under normoxia for 3 h or subjected to hypoxia/reoxygenation (H/R - grey zone) in the absence (-) or presence of eRNA. For all panels: Data represent mean ± SD (n = 6, independent experiments per group); exact p-value is shown or ns= not significant. Statistical significance was determined by one-way ANOVA with Bonferroni's post hoc test, as appropriate.

pattern similar to wild-type cells: LDH release increased from 27.8 ± 10.1 % of control under normoxia to 46.2 ± 9.3 % following H/R (*vs.* normoxia; p = 0.0103), and was further elevated upon eRNA treatment (62.7 ± 8.0 % of control; p < 0.0001 *vs.* normoxia, p = 0.0207 vs. H/R) (Fig. 5**D**). Accordingly, TNF-R2 likely does not play a critical role in eRNA-mediated cell death. Moreover, the consistent increase in LDH release following H/R across all genotypes highlights the presence of TNF-independent mechanisms - likely involving oxidative stress and mitochondrial dysfunction - that significantly contribute to cardiomyocyte injury.

2.6. In vitro RNase1-induced cardioprotection is linked to TNF-receptor-1 activation, while CsA induces cardioprotection independently of TNF-signaling

To investigate the cytoprotective effects of RNase1 and CsA on reoxygenation-induced cell death in cardiomyocytes, we measured LDH release into the supernatant following the induction of hypoxia/reoxygenation (H/R) in cardiomyocytes derived from WT, TNF-α-/-, TNF-R1-/-, and TNF-R2-/- mice. In WT cardiomyocytes (Fig. 6**A**), H/R significantly increased LDH release (43.8 ± 9.5 % of control), and this was significantly reduced by RNase1 (22.0 ± 6.6 % of control; p = 0.0003 *vs.* H/R), CsA (23.8 ± 7.6 % of control; p = 0.0009), or their combination (9.3 ± 5.2 % of control; p < 0.0001). Notably, combined RNase1 +CsA treatment led to a further significant reduction compared to RNase1 (p = 0.0459) or CsA alone (p = 0.0173), indicating a synergistic protective effect. No significant difference was observed between RNase1 and CsA treatments alone (p > 0.99).

In TNF-α-/- cardiomyocytes (Fig. 6**B**), LDH release increased after H/R (45.2 ± 9 % of control). CsA (29.5 ± 7.8 % of control) and RNase1 +CsA (25.17 ± 7.9 % of control) significantly reduced LDH release compared to H/R alone (p = 0.0222 and p = 0.0027, respectively), whereas RNase1 alone had no significant effect (45.5 ± 8.3 % of control, p > 0.99). Compared to RNase1, CsA conferred significantly greater protection (p = 0.0189), and importantly, the combination RNase1 +CsA provided a significantly enhanced protection compared to RNase1 alone (p = 0.0023). However, no additional reduction was observed when comparing co-treatment with CsA (p > 0.99), suggesting that while CsA drives the major protective effect, RNase1 contributes only partially, with its synergistic potential constrained by the absence of TNF-α.

In TNF-R1-/- cardiomyocytes (Fig. 6**C**), H/R-induced LDH release (40 ± 12 % of control) was significantly reduced by CsA (24.5 ± 7.9 % of control; p = 0.0459), but not by RNase1 (45.5 ± 8.3 %; p > 0.99). RNase1 +CsA (26 ± 9 % of control) significantly reduced LDH release compared to H/R (p = 0.0106). Interestingly, CsA alone was significantly more effective than RNase1 (p = 0.0054), and co-treatment was also superior to RNase1 alone (p = 0.0104), while no significant difference was found compared to CsA alone (p > 0.99), indicating a possible role of TNF-R1 in mediating the synergistic effects observed in WT cells.

In TNF-R2-/- cardiomyocytes (Fig. 6**D**), H/R-induced LDH release (41 ± 14 % of control) was significantly reduced by RNase1 (20 ± 6.2 % of control; p = 0.0039), CsA (23.3 ± 8 % of control; p = 0.0174), and RNase1 +CsA (12.3 ± 4 % of control; p = 0.0001). Notably, co-treatment with RNase1 +CsA led to a further significant reduction compared to RNase1 alone (p = 0.0364) or CsA alone (p = 0.0156), indicating a synergistic protective effect. No significant difference was observed between RNase1 and CsA monotherapies (p > 0.99), suggesting that TNF-R2 is not essential for the observed synergy between RNase1 and CsA.

2.7. RNase1 administration at the onset of reperfusion prevents eRNA-induced myocardial damage in vivo

The protective effect of RNase1, CsA, and their combination (RNase1 +CsA) against eRNA-induced myocardial damage was tested in an *in vivo* acute cardiac I/R model. WT mice were subjected to 45 min of coronary occlusion followed by 2 h of reperfusion[35,54]. Intravenous boluses of RNase1 (100 µg/mouse), CsA (10 mg/kg), a combination of RNase1 and CsA, or buffer control (NaCl) were administered 5 min prior to the reperfusion period [55]. Myocardial

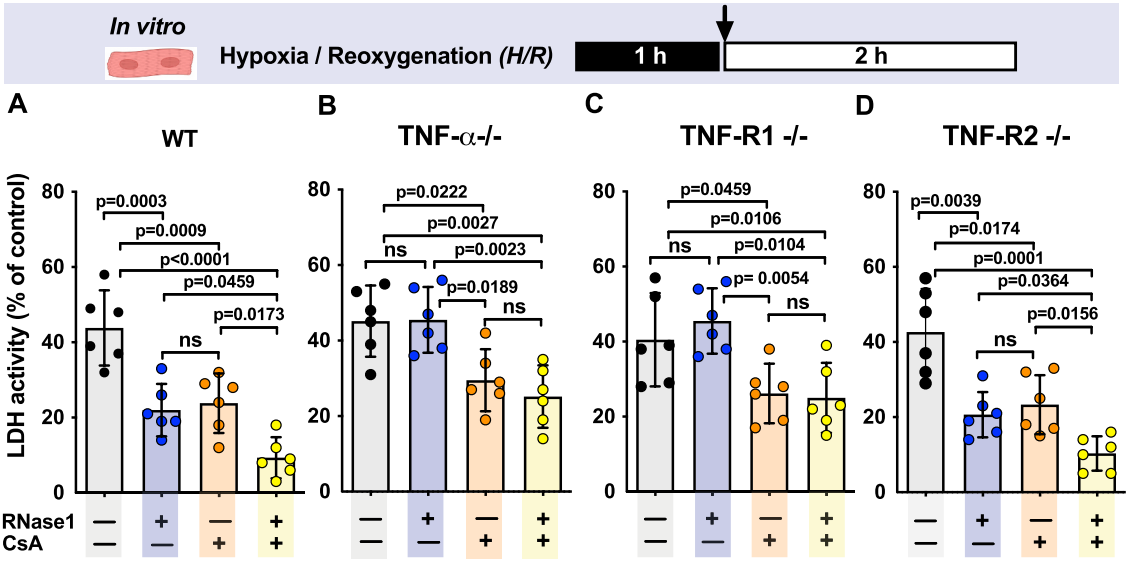

Fig. 6. Cytoprotective influence of RNase1 and CsA on reoxygenation-induced cell death. Following the induction of the cardiomyocyte hypoxia/reoxygenation model, the release of LDH from cardiomyocytes was quantified in the supernatant from (A) wild-type (WT), (B) TNF-α-/- mice, (C) TNF-R1-/- mice, or (D) TNF-R2-/- mice in the absence (-) or presence of RNase1(10 µg/ml) and/or CsA (1 µmol/L). Where indicated, RNase1 and/or CsA were introduced into the medium at the onset of reoxygenation and were present throughout reoxygenation phase. For clarity, treatment groups are represented as follows: Control (grey bar), RNase1 (blue bar), CsA (orange bar), and RNase1 +CsA combination (yellow bar). For all panels: Data represent mean ± SD (n = 6, independent experiments per group); exact p-value is shown or ns= not significant. Statistical significance was determined by one-way ANOVA with Bonferroni's post hoc test, as appropriate.

infarct size was determined after 2 h reperfusion by dual staining with 2,3,5-TTC / Evans blue to delineate viable myocardium and marking of non-at-risk regions of the heart, respectively. Infarct size, expressed as a percentage of the area at risk (IS/AAR, %), was significantly reduced in the RNase1-treated group compared to the buffer control (NaCl) group (32.3 ± 6 *vs.* Control $= 50.9 \pm 6$ %; $p = 0.0039$). Similarly, CsA-treated mice showed a significant reduction compared to controls (27.8 ± 8; $p < 0.0001$), while RNase1 +CsA (19.2 ± 7 %; $p < 0.0001$) combination therapy further reduced infarct size slightly, showing a possible synergistic effect compared to controls. This combination also resulted in significantly smaller infarcts compared to RNase1 alone ($p = 0.0006$) and to CsA alone ($p = 0.0416$). There was no statistically significant difference between RNase1 and CsA monotherapies ($p = 0.8537$), suggesting that both are similarly effective as single agents. Representative images (scale bar = 5 mm) clearly illustrate the infarct size differences among treatment groups. It is important to note that the area at risk was similar among all groups, indicating that the initial extent of myocardial ischemia was comparable ($p > 0.99$; ns between groups) (Fig. 7 **A-C).** Moreover, the ROS content in I/R hearts (200 ± 37 AU/μm^2) was significantly reduced upon treatment with RNase1 (145 ± 22 AU/μm^2; $p = 0.0015$) CsA (146 ± 23 AU/μm^2; $p < 0.0001$) or a combination of both (106 ± 36 AU/μm^2; $p < 0.0001$), highlighting their important role in attenuating oxidative stress in the injured heart **(**Fig. 7**D).** Overall, these results indicate that both RNase1 and CsA independently protect the heart from I/R-induced damage, and their combination offers an enhanced protective effect.

3. Discussion

In the present study, we provide novel mechanistic insights into the early phase of cardiac I/R injury, driven by the endogenous eRNA/RNase system. The eRNA-dependent, TNF-α-related pathways identified here may not be restricted to ischemic heart disease but could also extend to ischemia-induced damage in other organs or tissues. Furthermore, interventions with TACE inhibitors (such as TAPI) or RNase1 may offer promising new strategies for general cytoprotection. Our data support a previously unrecognized, reciprocal and deleterious interaction between eRNA and TNF-α in myocardial I/R injury. The rationale for studying the role of eRNA as an early alarm signal in ischemic heart disease was based upon our previous findings that these poly-anionic compounds promoted arterial thrombosis [56], and induced the release of cytokines that led to increased vascular permeability, I/R injury [34,35] and oedema formation *in vivo*[57]. Clinical validation from our previous study further supported this concept: in a cohort of patients undergoing cardiac surgery, we observed a parallel and significant increase in circulating eRNA and TNF-α levels after aortic declamping, particularly in coronary sinus blood [26,34]. Under ischemic conditions, eRNA significantly downregulated the expression of antioxidant enzymes, strongly suggesting that it contributes to the impairment of the endogenous protective mechanisms under stress conditions [35]. The effects of eRNA were largely inhibited by RNase1, placing RNase1 as a prominent vessel-protective agent[58]. The significant increase in RNase1 following remote ischemia preconditioning in patients, without affecting normal cardiac function parameters or inflammation [26,34], further supports the relevance of this molecular system under investigation.

Acute elevation of eRNA levels, both free and associated with microvesicles [36], was observed at the onset of reperfusion in the isolated rat heart model and in hypoxia-exposed cardiomyocytes. This finding aligns with a recent report showing the release of tissue factor-bearing microvesicles from cardiomyocytes under inflammatory conditions [59]. Likewise, increased plasma concentrations of eRNA were noted in acute models of vessel stenosis and chronic atherosclerosis in mice [60]. Upon induction of I/R, an initial reperfusion-dependent washout of eRNA, along with cardiomyocyte-specific markers like CK and troponins, was followed by a second peak of eRNA, likely

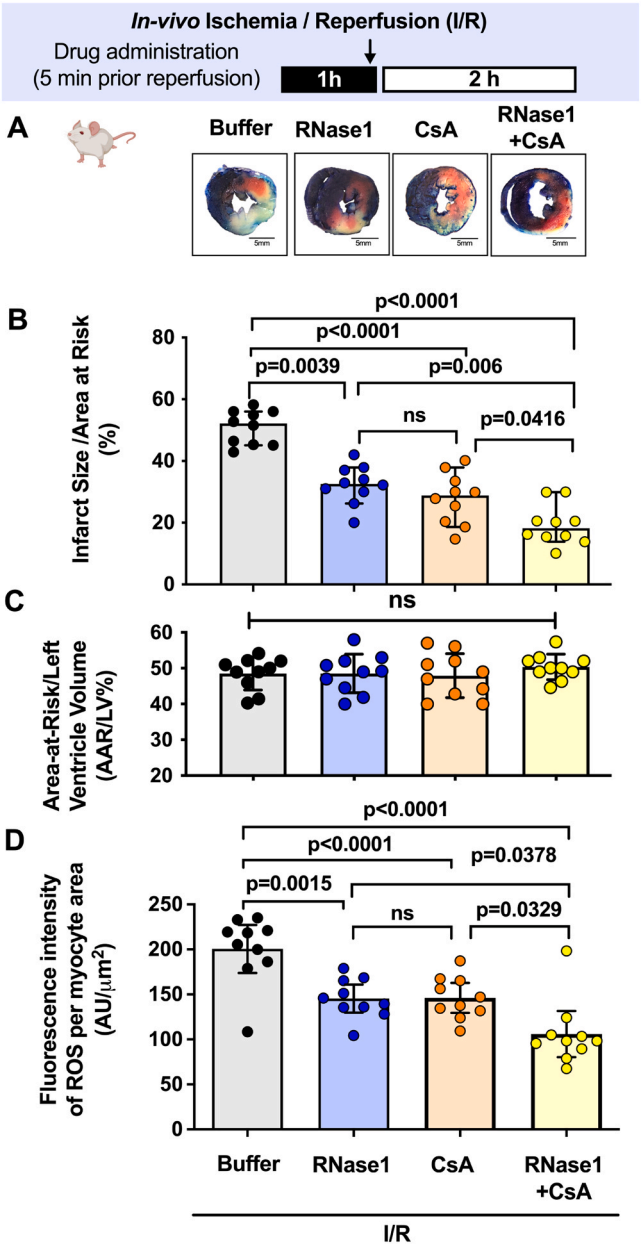

Fig. 7. RNase1 administration at the onset of reperfusion prevented eRNA-induced myocardial damage *in vivo*. Study protocol. Following the induction of the *in vivo* acute cardiac I/R model in WT mice, infarct size (expressed as percentage of area at risk) was quantified after coronary occlusion (45 min) followed by 2 h reperfusion. As indicated by the arrow, 5 min prior to the reperfusion period, treated mice received an intravenous bolus of buffer control (NaCl), RNase1 (100 μg/mouse), CsA (10 mg/kg) or a combination of RNase1 and CsA respectively; values represent mean ± SD (n = 10 mice per group). Scale bar, 5 mm. (A) Representative pictures show myocardial infarct size in the heart sections indicated by dual staining with 2,3,5-TTC (1 %) and Evans blue (1 %). (B) Myocardial infarct size quantification, measured by Infarct Size / Area at Risk (%) when compared to buffer control (NaCl) in adult WT mice subjected to *in vivo* IRI. (D) Microslices obtained from mice hearts of the groups described were analyzed by immunofluorescent staining. Quantitative analysis of ROS (dihydroethidium) production was performed; values represent mean ± SD (n = 3 hearts). For clarity, treatment groups are represented as follows: Control (grey bar), RNase1 (blue bar), CsA (orange bar), and RNase1 +CsA combination (yellow bar). For all panels: Data represent mean ± SD (n = 6, independent experiments per group); exact p-value is shown or ns= not significant. Statistical significance was determined by one-way ANOVA with Bonferroni's post hoc test, as appropriate.

originating from cardiomyocytes and/or fibroblasts [35], the two major cell types in the heart. Unlike CK, troponins, or LDH, eRNA continued to be released into the perfusate over a prolonged period, potentially acting as a cell-damaging factor through direct or indirect effects on cell functions. To block the direct or indirect effects of eRNA, RNase1 was applied in experimental models *in vitro* in comparisons made to RNase inhibitor treatment, which effectively and immediately inhibited any residual endogenous RNase1. Collectively, these results from three distinct experimental I/R injury models, coupled with the positive correlation between circulating eRNA and serum CK in STEMI patients, provide strong evidence for the significant role of the eRNA/RNase system in ischemic cardiac disease and highlight the tissue-protective effects of RNase1.

Recent findings have also identified the DAMP "extracellular RIPK3" as a significant contributor to cardiac I/R injury [28], suggesting that inflammatory mediators may interact with the eRNA/TNF-α signaling pathways, potentially exacerbating tissue damage during ischemic events. Since eRNA, as a DAMP, in association with inflammatory processes, may provoke the release of TNF-α via a proteolytic shedding reaction involving the metalloproteinase TACE [41], we tested whether this mechanism would apply to the model of I/R injury as well. While a significant elevation of TNF-α was induced under I/R in the isolated heart model as well as under hypoxic conditions in cardiomyocytes, the presence of RNase1 mitigated TNF-α shedding [61].

In this context, recent data demonstrate that ribosomal eRNA can synergize with Toll-Like Receptor 2 (TLR2) ligands to amplify inflammatory cytokine release via TLR2/NF-κB signaling [62], although the potential involvement of cytosolic RNA sensors such as PKR, MDA5, or RIG-I in recognizing endogenous eRNA remains to be determined. This supports a broader role for eRNA in sterile inflammation and aligns with our current findings in the I/R setting**,** where eRNA functions not only as a DAMP but also as a key amplifier of cytokine signaling. Although our study provides important insights into the role of eRNA in TNF-α shedding via TACE activation, the underlying intracellular signaling mechanisms remain to be fully elucidated. As we have demonstrated, eRNA induces TACE-dependent TNF-α release from cardiomyocytes in a manner dependent on intact RNA, which can be prevented by RNase1 **(**Fig. 8**A)**. However, the precise pathways leading to TACE activation, particularly involving MAPK, Akt, and NF-κB signaling, warrant further investigation. In our previous work, we identified these signaling cascades as critical mediators of eRNA-induced TACE activation in other cell types [51]. Given the potential relevance of these pathways in cardiomyocytes and infiltrating immune cells during myocardial I/R injury, we propose that future cardiac-specific studies should investigate the role of MAPK, Akt, and NF-κB signaling in eRNA-mediated TACE activation to further understand the mechanisms underlying this process.

Since TNF-α largely recapitulates the adverse effects of eRNA during I/R in the isolated rat heart and in hypoxic cardiomyocytes (particularly with respect to mPTP opening, cardiomyocyte contracture and cytokine release), it seems likely that these factors influence each other in their detrimental effects. Indeed, TNF-α directly promoted eRNA release, specially under hypoxic conditions, further enhancing TNF-α release and establishing a vicious cycle that leads to cardiomyocyte death. Importantly, inhibiting TACE with protease inhibitors prevented TNF-α shedding and mitigated subsequent pathological outcomes, such as LDH release. Thus, TACE inhibitors closely mimic the protective effect of RNase1 in cardiac I/R injury, and both strategies appear to offer promising approaches for tissue protection in ischemic heart disease. These therapies could be applied during acute percutaneous coronary intervention in STEMI patients to prevent or reduce cardiac tissue injury. Consistent with this protective profile, administration of RNase1 prevented LDH release during I/R as a general marker for necrotic cell death. In addition to its protective role against mPTP opening RNase1 significantly reduced ROS levels in cardiomyocytes (both *ex vivo* and *in vivo*) and, most importantly, led to a marked reduction in infarct size and preservation of tissue architecture. These findings provide conclusive evidence that RNase1 protects multiple physiological parameters, underscoring its causative relation in RNA-hydrolysis. We demonstrate that eRNA stimulates TNF-α shedding from cardiomyocytes under normoxic and hypoxic conditions, a response that is abrogated by RNase1. In turn, TNF-α promotes eRNA release, establishing a functionally reinforcing feedback loop **(**Figs. 2**A,** 3**A–C)**. Although we did not perform time-resolved or sequential blockade experiments, the functional interdependence between eRNA and TNF-α is clear: both sensitize cardiomyocytes to mPTP opening, and these effects are reversed by RNase1 or anti-TNF-α **(**Figs. 2**B,** 2**C,** 3**F)**. This loop appears pathophysiologically relevant.

While the primary focus of this study was on the direct cardiomyocyte-mediated mechanisms of eRNA and TNF-α toxicity, it is important to consider that TNF-α can also influence coronary vascular tone, potentially contributing to no-reflow phenomenon or microvascular dysfunction during reperfusion [6,63,64]. Although our Langendorff data showed no significant change in coronary flow with TAPI treatment, suggesting that improved perfusion was not the primary driver of protection in that model, a potential vascular component of the eRNA/TNF-α axis in the intact organism represents an interesting avenue for future research.

Exogenous eRNA administration significantly increased infarct size **(**Fig. 2**E),** and our previous clinical study showed that both eRNA and TNF-α are markedly elevated in coronary sinus blood during cardiac surgery. Notably, remote ischemic preconditioning (RIPC) increased endogenous RNase1 and reduced both mediators, highlighting the therapeutic potential of modulating this axis [34]. These findings provide strong functional evidence for a self-reinforcing eRNA–TNF-α circuit that drives myocardial damage and support the therapeutic targeting of this pathway with RNase1.

To investigate whether additional cardioprotective effects could be achieved by targeting distinct cell death pathways, we also evaluated CsA, a well-characterized inhibitor of the mPTP - a key contributor of reperfusion-induced cardiomyocyte death. CsA has demonstrated consistent efficacy in preclinical models by reducing infarct size and preserving cardiac function through stabilization of mitochondrial integrity during reperfusion [65]. However, its failure to show clinical benefit in large randomized trials, such as CIRCUS, has raised concerns about its translational potential [66]. Possible contributing factors include inadequate delivery to ischemic myocardium, variability in CYP3A4-mediated metabolism, and off-target effects such as calcineurin inhibition [67]. Despite these limitations, CsA remains a well-established experimental tool to confirm the contribution of mitochondrial permeabilization to I/R injury, with recent studies reinforcing its protective effects when administered at the onset of reperfusion, even in settings such as heart transplantation after circulatory death heart models [68]. We acknowledge that Fig. 2C does not include a combined eRNA + RNase1 + CsA group, which limits conclusions regarding potential additivity at the level of mPTP opening. This limitation is important to note; however, additivity was directly assessed in subsequent *in vitro* and *in vivo* experiments, where RNase1 and CsA co-treatment consistently provided enhanced cardioprotection compared to either agent alone.

Our data also demonstrate that RNase1 and CsA provide significant cytoprotection against reoxygenation-induced cell death in cardiomyocytes. While both agents are effective individually across all tested genotypes, their combined effect is most pronounced in WT cells. The absence of TNF-α or TNF-R1, but not TNF-R2, appears to diminish the synergistic benefits of RNase1 and CsA co-treatment. However, CsA retained its protective effect, suggesting that TNF signaling pathways may play a role in mediating their combined cytoprotective effects. In an *in vivo* I/R murine model, the administration of RNase1, CsA, or their combination at the time of reperfusion significantly reduced myocardial infarct size. Notably, the combination of RNase1 and CsA suggest a possible synergistic protective effect, highlighting their potential for

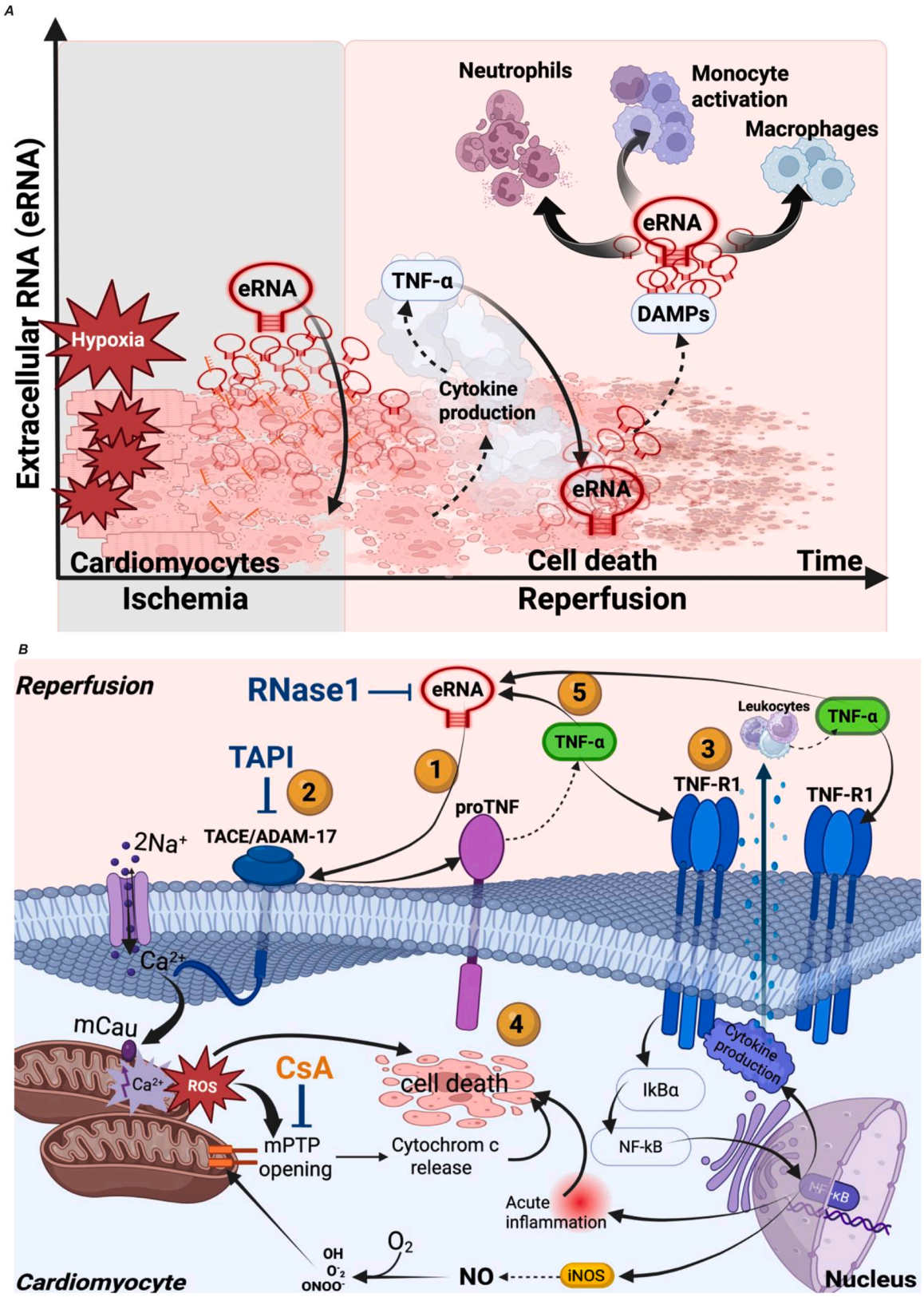

(caption on next page)

Fig. 8. Proposed mechanism of eRNA–TNF-α interplay mediating cardiomyocyte injury during ischemia/reperfusion (I/R) and the protective effects of RNase1 or TACE inhibition. (A) During ischemia, hypoxic stress triggers the release of extracellular RNA (eRNA) from injured cardiomyocytes. Upon reperfusion, eRNA levels markedly increase and act as danger-associated molecular patterns (DAMPs), promoting monocyte activation, macrophage-mediated cytokine release, and neutrophil recruitment. These responses further enhance inflammation and TNF-α production, creating a positive feedback loop. (B) Mechanistically, eRNA [1] induces the activation of TNF-α converting enzyme (TACE/ADAM17) [2], which cleaves membrane-bound pro-TNF-α into its soluble, active form. TNF-α then binds to TNF-R1 [3], activating NF-κB signaling, inflammatory gene expression, and inducible nitric oxide synthase (iNOS). Simultaneously, this signaling cascade contributes to mitochondrial calcium overload, ROS accumulation, and mitochondrial permeability transition pore (mPTP) opening, culminating in cytochrome c release and cell death [4]. eRNA induces TNF-α release, which in turn triggers further eRNA release, forming a self-amplifying inflammatory feedback loop [5]. RNase1-mediated hydrolysis of eRNA and TAPI (a TACE inhibitor) interrupts this cascade, representing a promising strategy to reduce acute inflammation and cardiomyocyte death. Combined administration of RNase1 and CsA yields synergistic cardioprotection, effectively interrupting both upstream inflammatory signaling and downstream mitochondrial death pathways.

mitigating myocardial damage following I/R injury.

These findings support the view that CsA and RNase1 act via distinct mechanisms: CsA stabilizes mitochondria by inhibiting mPTP opening, whereas RNase1 neutralizes eRNA and reduces TNF-mediated inflammatory signaling. The enhanced protection observed with RNase1 +CsA in TNF-α-/- and TNF-R1-/- cardiomyocytes likely reflects a shift in mechanism. While RNase1 alone is ineffective in these genotypes - where TNF-dependent inflammatory injury is absent - CsA's inhibition of mPTP may unmask a secondary benefit of RNase1. Specifically, eRNA hydrolysis by RNase1 generates nucleotides such as adenosine, which may activate purinergic signaling pathways (e.g., A1 receptor [69]) that reduce mitochondrial injury independently of TNF-α. Although a prior study showed that the non-selective adenosine receptor antagonist 8-sulfophenyltheophylline (8SPT) did not alter RNase1-mediated infarct size reduction in the Langendorff model [35], this does not exclude context-dependent, TNF-independent purinergic contributions under conditions of preserved mitochondrial integrity. Thus, RNase1 may exert dual, inflammation- and mitochondria-modulating effects, and this novel mechanism warrants further investigation. Their combined benefit suggests that mitochondrial dysfunction and sterile inflammation are parallel and additive contributors to I/R injury. Moreover, RNase1 administration during ischemia reduces ROS production and preserves myocardial architecture in both *in vivo* and *ex vivo* models of cardiac I/R injury [35]. This effect was associated with decreased nuclear ROS accumulation and increased expression of antioxidant enzymes such as peroxiredoxin 3 and mitochondrial superoxide dismutase (SOD2). In the present study, we expand these findings by showing that RNase1 administration at reperfusion significantly reduces ROS generation *in vivo* (Fig. 8**B**). Further studies are warranted to explore the underlying mechanisms and potential clinical applications of these treatments in cardiovascular diseases.

In summary, while further work is needed to characterize the kinetics and regulation of this circuit, our findings establish a mechanistic rationale for targeting the eRNA–TNF-α axis in myocardial injury, with RNase1 as a promising intervention point. The paradoxical increase in cytotoxicity in the TNF-R2-/- model in response to eRNA exposure presents intriguing insights into the complex roles of TNF-α receptors in I/R injury. Previous studies have highlighted the dual nature of TNF-α signaling, where TNF-R1 is typically associated with pro-inflammatory and pro-apoptotic responses, while TNF-R2 has been implicated in anti-inflammatory and tissue-protective roles [70–72]. Our findings suggest that the balance between these receptors may be more intricate than previously recognized, with TNF-R2 potentially serving as a regulator of TNF-R1 signaling in the context of eRNA exposure. The dysregulated inflammatory response observed in the absence of TNF-R2 underscores the potential for therapeutic targeting of this balance in clinical settings, such as myocardial infarction or other ischemic diseases. Moreover, the role of eRNA in modulating TACE activation and subsequent TNF-α release further complicates the interpretation of TNF-α signaling. While TNF-α signaling via TNF-R1 alone may suffice to drive injury under ischemic conditions, eRNA exposure may enhance this response by promoting TACE-mediated cleavage of membrane-bound TNF-α. This suggests that eRNA, a key DAMP, may act as an amplifier of ischemic injury, particularly in tissues with an imbalanced TNF-α receptor signaling pathway **(**Fig. 8**).** Future studies exploring the mechanistic underpinnings of eRNA-TACE-TNF-α interactions, as well as the specific roles of TNF-R1 and TNF-R2, are crucial for identifying novel therapeutic targets to mitigate I/R injury. Integrating these novel strategies into clinical practice can potentially improve the prognosis and quality of life for patients suffering from acute myocardial infarction and other related cardiovascular disease conditions**.**

4. Limitations of the study

In this study, we primarily focused on the roles of eRNA and TNF-α in myocardial I/R injury, specifically in myocardial and vascular endothelial cells. However, this approach does not encompass other critical factors involved in STEMI, such as the contributions of platelets, leukocytes [73], arachidonate 12-lipoxygenase [74] and the local formation of NETs [75]. These elements, which also play a significant role in cardiac injury, can be modulated through the TRAIL-DR5 signaling pathway [76]. Additionally, while our data focus on TNF-α release, future studies should broaden cytokine profiling to include IL-6, IL-1β, and chemokines released by cardiomyocytes during H/R and *in vivo* I/R. Prior work has shown that eRNA induces a robust pro-inflammatory response, including M1 macrophage polarization and upregulation of TNF-α, IL-6, IL-1β, and IFN-γ, underscoring its role as a potent DAMP [40,60].This study did not include additional *in vivo* cardiac functional parameters beyond infarct size and LDH release. However, cardiac function following RNase1 treatment during the ischemic phase has been previously reported by our group, demonstrating preserved ventricular contractility and relaxation [35]. Importantly, infarct size remains a robust and translational endpoint, as underscored by the recent IMPACT multicenter study, which reaffirmed TTC/Evans Blue staining —primarily indicative of necrosis [77]— as the gold standard in preclinical models [78]. However, myocardial I/R injury involves other regulated cell death pathways—such as ferroptosis, necroptosis, and pyroptosis—that were not assessed here [79]. Future studies should include these pathways to better understand the full scope of eRNA-induced cardiomyocyte death in myocardial infarction. Additionally, further preclinical studies are required to evaluate the combination of RNase1 with other cardioprotective agents, particularly those targeting pro-inflammatory pathways independently of TNF-R1, such as NLRP3 inflammasome inhibitors [80,81], sirtuins [82], and Ca^{2+} /calmodulin-dependent protein kinase II (CaMKII) [28,83], as well as pathways related to succinate metabolism [19,20].

Moreover, an unexplored but potentially critical mechanism involves the generation of nucleotide byproducts from RNase1-mediated eRNA degradation. The lack of direct quantification of such byproducts - adenosine, ATP, or AMP - limits our ability to assess the contribution of purinergic signaling to the observed cardioprotective effects. Since

adenosine is known to activate A1 receptors and mitigate mitochondrial injury and mPTP opening, future studies should include nucleotide profiling and A1 [69] receptor blockade to clarify whether adenosine-mediated mechanisms contribute to RNase1's protection, particularly in TNF-deficient contexts.

Another important limitation of our study is the use of supra-physiological concentrations of eRNA *in vitro* (10 μg/ml) and *in vivo* (15 μg/mouse). While these doses are based on previous work showing their ability to robustly activate inflammatory signaling without cytotoxicity [40,51], they exceed typical systemic levels found in STEMI patients. Nevertheless, they were intended to mimic localized micro-environments - such as ischemic myocardium - where transient eRNA accumulation may be significantly higher, particularly under conditions that promote the release of DAMPs. Previous studies have shown that coronary sinus eRNA levels during cardiac surgery can exceed 200–600 ng/ml [26,34], supporting this rationale. Nevertheless, future studies should assess the bioactivity of eRNA under more physiological conditions, such as by testing the effects of plasma from STEMI patients collected post-PCI on cardiomyocyte inflammation and viability.

Although this study focused exclusively on males, the mechanistic pathways investigated—particularly the eRNA-TNF-α signaling axis—are not inherently sex-specific, based on existing evidence. Moreover, our study aims to focus exclusively on eRNA-TNF-α signaling axis in cardioprotection, excluding the effect of estrogen, which is a well-known protective of myocardium during ischemia [84]. By understanding the role of each protective mechanism, we will be able to evaluate in future research the sex-specific differences in the therapeutic efficacy of RNase1 and to confirm the broader applicability of these findings. Investigating these interactions will enhance our understanding of recovery from myocardial injury and may lead to more effective therapeutic strategies.

While this study presents significant findings on the correlation between eRNA levels and CK_{max} serum concentration in STEMI patients, it is important to acknowledge the limitations of the current data. Although functional outcome data such as left ventricular ejection fraction (LVEF) was not collected in this study, eRNA levels were positively correlated with CK_{max}, which serves as a surrogate marker for infarct size. This correlation suggests that eRNA may provide valuable insights into cardiac injury severity, although further investigation is needed to better understand the full spectrum of clinical implications.

A key limitation of this study is the absence of detailed clinical data, such as LVEF, from the STEMI patient cohort. Functional outcome measures like LVEF would have strengthened the interpretation of how molecular alterations relate to cardiac performance following myocardial I/R injury. Although this study centers on the acute phase of I/R injury, future investigations should incorporate comprehensive clinical metrics, including LVEF and relevant biomarkers, to enable a more robust correlation between molecular mechanisms and long-term cardiac function in affected patients. Despite this limitation, the therapeutic potential of RNase1 remains promising. Notably, the IgG-Fc-fusion protein of RNase1 (RSLV-132), which has a prolonged half-life (19 days), has been tested safely in phase II clinical trials. These advances support the feasibility of testing RNase1-based therapies in cardiovascular patients, particularly in the context of I/R injury [85]. Based on these promising studies it is expected that this product will be tested in cardiovascular patients, particularly in situations of myocardial infarction and prevention of I/R injury as well.

5. Conclusion

Our study highlights the critical roles of eRNA and TNF-α in myocardial I/R injury. eRNA acts as a DAMP, serving as a robust biomarker and mediating cardiomyocyte death through TNF-α/TNF-R1 signaling. We also demonstrate that RNase1 and CsA offer significant cytoprotection against reoxygenation-induced cell death in cardiomyocytes, with their combined effect being most pronounced in wild-type cells. The synergistic benefits of RNase1 and CsA are diminished in the absence of TNF-α or TNF-R1, indicating the involvement of TNF signaling pathways. *In vivo*, the combination of RNase1 and CsA provided significantly greater cardioprotection than either agent alone, despite the comparable levels of protection observed with each monotherapy. These findings support the development of novel therapeutic strategies that simultaneously target intracellular (mitochondrial) and extracellular (inflammatory) pathways to mitigate myocardial I/R injury. Such multi-target approaches may be particularly beneficial in clinical contexts marked by heightened inflammation or extracellular nucleic acid accumulation. Incorporating agents like RNase1 or TACE inhibitors into clinical protocols could potentially enhance patient outcomes by reducing infarct size and preserving myocardial function. Future clinical trials will be essential to evaluate the safety, efficacy, and translational relevance of these combinatorial therapies.

6. Methods

6.1. Statistical analysis

Statistical analyses were conducted using GraphPad Prism version 10.3.1 for macOS (GraphPad Software, La Jolla, CA, USA; www.graphpad.com). Data are presented as mean ± standard deviation (SD or mean ± SEM, as specified in each figure panel. Statistical significance is shown as $*p < 0.05$, $**p < 0.01$, $***p < 0.001$, $****p < 0.0001$, and ns=not statistically significant. In some cases, exact *p*-values are shown directly on the graphs. For comparisons between two groups, two-tailed Statistical significance was determined using one-way ANOVA followed by Bonferroni's post hoc test for comparisons among multiple groups, or unpaired Student's *t*-test for comparisons between two groups, as appropriate. For specific comparisons, the Mann–Whitney *U* test was applied. Sample size was calculated based on preliminary experiments, assuming an α of 0.05 and a power (1–β) of 0.8. Data were not excluded from the analysis. Animals were randomly assigned to experimental groups, and investigators were blinded to group allocation. The number of biological replicates (n) is indicated in the respective figure panels or legends.

6.2. Sex as a biological variable

This study exclusively involved male subjects in both the human and animal models. Biological sex significantly influences cardiac outcomes, with extensive evidence showing that females consistently exhibit smaller infarct sizes compared to males across various species [86]. In the human cohort, male STEMI patients were selected to minimize variability introduced by hormonal fluctuations, as estrogen and other sex hormones are known to modulate inflammatory and reperfusion-related processes in myocardial I/R injury [87–89]. Similarly, in the rodent models, male mice and rats were chosen supported by prior research demonstrating sex-based differences in the acute inflammatory response and myocardial injury, with males exhibiting more consistent and reproducible responses in these contexts [90,91].

6.3. Study population

A total of 23 male patients aged 18 years or older were included in the study and categorized into two groups: a) *Patients:* Twelve patients with STEMI treated with PCI with stipulations that they presented within 12 h after the onset of chest pain, exhibited ST-segment elevation of more than 0.1 mV in two contiguous leads, and for whom the clinical decision was made to treat with PCI [66]. b) *Matched-Control Patients:* Eleven patients who did not have STEMI but presented with chest pain, without a prior chest pain consultation or IHD diagnosis before 2010 or within 2 weeks after the index date, were selected from our database, using inclusion and exclusion criteria similar to those applied in previous work with the General Practice Research Database [92]. Data were

anonymized prior to analysis. Plasma eRNA levels were measured using a quantitative assay. The mean eRNA levels for control and STEMI patients were recorded [34]. Serum CK_{max} levels were quantified using an enzymatic assay at the study centre. The highest CK levels recorded 2 hr post-PCI were used for analysis [93]. All patients provided written informed consent. Samples were used exclusively for research purposes. All protocols involving human material were approved by the Ethics Committee of the Medical Faculty of Justus Liebig University Giessen, Germany (Ref. No. 74/08), and conducted in accordance with the principles of the Declaration of Helsinki.

6.4. Ethics and animal housing

This study utilized *in vitro*, *ex vivo*, and *in vivo* models of I/R injury. For *in vitro* or *ex vivo* experiments, C57BL/6 J, TNF-α knockout (TNF-α-/-), TNF receptor 1-knockout (TNF-R1-/-), and TNF receptor 2 knockout (TNF-R2-/-) mice or Wistar rats were used. Both the mice and rats were housed at the animal care facility of Justus-Liebig-University in Giessen, Germany, under standardized conditions. For *in vivo* studies, male C57BL/6 J mice (aged 8–14 weeks, body weight ~24–30 g) were used in compliance with ethical guidelines approved by the Singapore Health Services (SingHealth) Institutional Animal Care and Use Committee (IACUC) (#2020/SHS/1563). A limitation to the generalisability of the study is that it did not consider gender/sex issues. All animals were housed in pathogen-free environments and treated in accordance with the Guide for Care and Use of Laboratory Animals (Eighth Edition), published by the US National Institute of Health Publications (NIH publication no. 85–23, revised 1996). All animals were treated in accordance with Animal Research: Reporting of *in vivo* Experiments (ARRIVE) guidelines, ensuring humane care and minimizing pain, distress, and any potential misuse [94]. Experimental conditions are outlined in the corresponding legends to Figures.

6.5. Murine model of myocardial I/R

The established *in vivo* experimentation was carried out exactly as previously described [54,78,95]. Briefly, eight to ten-week-old male C57Bl/6 J mice were anesthetized by intraperitoneal injection with a combination of ketamine, xylazine and atropine (0.01 ml/g, final concentration of ketamine, xylazine and atropine were 10 mg/ml, 2 mg/ml and 0.06 mg/ml, respectively) and body temperature was maintained at 37°C. Mice underwent 1 h coronary occlusion followed by 2 h reperfusion. Animals were treated with eRNA (15 μg/mouse), RNase1 (Fermentas, 100 μg/mouse), RNase Inhibitor (RiboLock, Fermentas, 80 U/mouse) or Cyclosporine-A (CsA, Calbiochem, 10 mg/kg [96]). Successful LAD coronary artery occlusion was confirmed by the presence of ST elevation and decreases in arterial blood pressure. At the end of the reperfusion, the heart was isolated and the aortic root was cannulated and used to inject 2,3,5-triphenyltetrazolium chloride (TTC, 5 ml of 1 %) in order to demarcate the infarcted tissue. The LAD coronary artery was then re-ligated and Evans blue dye (2 ml of 0.5 %) was perfused to delineate the area at risk. The heart was frozen and sectioned perpendicularly to the long axis (1–2 mm thick). The slices were then transferred to 10 % neutral buffer formalin for 2 hr at room temperature to stabilize the staining. Area at risk and infarct size were determined by computerized planimetry using the NIH software Image, following incubation with 10 % formaldehyde for 2 hr at room temperature. Area at risk was expressed as a percentage of the left ventricle and infarct size was expressed as a percentage of the area at risk. Quantification of the infarcted area were done as previously described [35,78].

6.6. Isolated Langendorff-perfused heart model

Experiments were performed on isolated hearts from Wistar rats (10–12 weeks old; weighing 225–300 g) as previously described [35,97].

6.7. Isolation of adult mouse and rat cardiomyocytes

Ventricular heart muscle cells were isolated from 10 to 12-weeks old Wistar rats or C57BL/6 J, TNF-α-/-, TNF-R1-/-, and TNF-R2-/- mice as previously described [98,99]. Cardiomyocytes were seeded onto sterilized, laminin-coated coverslips and incubated in minimum essential medium (MEM - Gibco™) supplemented with 10 U/ml penicillin, 10 μg/ml streptomycin, and 5 % fetal calf serum, for use on the same day of isolation ($n > 200$ cells per group, pooled from 3–6 independent animals). Detailed group descriptions are indicated in the respective figure legends.

The following agents were used for stimulating cells: TNF-α from R&D, recombinant bovine RNase1 from Fermentas, RNase inhibitor (RiboLock) from Fermentas, Bay11–7082 (Bay) from ENZO Life Sciences, GM6001 from Millipore, TAPI from ENZO Life Sciences, CsA from Calbiochem or antibodies against TNF-α from Biozol at the indicated concentrations.

6.8. Preparation and characterization of eRNA

Total RNA was isolated from freshly isolated mouse cardiomyocytes using the MasterPure™ RNA Purification Kit (Epicentre Biotechnologies) following manufacturer instructions. Quantification was performed with a NanoDrop ND-2000 spectrophotometer (peqLab Biotechnologie GmbH). Based on our previously published work and as mentioned above, the eRNA extracted under these conditions is **predominantly composed of ribosomal RNA (rRNA),** particularly **intact 28S and 18S subunits,** as shown via capillary electrophoresis and bioanalyzer analysis [34,36,60]. These eRNA species have been functionally validated in prior studies as **bioactive DAMPs** capable of endothelial barrier disruption, inflammatory cytokine induction, and myocardial injury during I/R. Additionally, RT-PCR-based profiling of cell-type-specific transcripts confirmed the **cardiomyocyte origin** of eRNA in comparable models [35,40]. Given the reproducible biological activity and compositional stability of this RNA preparation in ischemic settings, it was used to mimic extracellular RNA exposure *in vitro* and *in vivo*. RNA was hydrolyzed by incubation with RNase1 (Fermentas®) for 1 hr at 37°C. Hydrolyzed RNA was always used in parallel assays at the same concentration as untreated RNA. The quality control of the total and hydrolyzed RNA was done using the 2100 Bioanalyzer with "Eukaryote total RNA Nano Assay" (Agilent Technologies). All chips were analyzed in duplicates.

6.9. Isolation of DNA for cardiomyocyte treatment

DNA was isolated with GenElute Mammalian Genomica DNA Miniprep Kit (Sigma-Aldrich) from confluent cultures of smooth muscle cells. Quality of total DNA was confirmed by electrophoresis on a 1 % agarose gel followed by ethidium bromide staining [100].

6.10. Quantification of cell death

Lactate dehydrogenase (LDH) activity in the Langendorff-perfusate was measured spectro-photo-metrically during the entire reperfusion period of 2 h [101]. LDH release into the cardiomyocyte-conditioned medium was assessed by a detection kit (Roche Diagnostics) [100,102].

6.11. TNF-α quantitation

Langendorff-heart perfusate and cardiomyocyte conditioned medium were collected and filtered through 0.2 μm filter to remove any residual debris. TNF-α production by heart tissue submitted to I/R or released from cardiomyocytes was assessed by enzyme-linked immunesorbent assay (ELISA) (Quantikine®, R&D Systems) according to manufacturer's protocol. Absorbance values for individual reactions were determined by VersaMax™ Microplate Reader (SoftmaxPro 3.0

processing).

6.12. Exposure of cardiomyocytes to hypoxia and reoxygenation (H/R)

Cardiomyocytes were subjected to hypoxia by placing the culture plates in a sealed hypoxic chamber (BBL™ GasPak™, BD Biosciences) within a standard cell incubator at 37 °C for 1 h [103]. After the hypoxic phase, the GasPak™ system was removed, and cells were reoxygenated under normoxic conditions (21 % O_2) in the same incubator for an additional 2 h. Pharmacological treatments were administered directly to the culture plates at the onset of reoxygenation - without changing the culture medium - to simulate reperfusion. At the conclusion of the reoxygenation period, both cells and supernatants were harvested for downstream analyses, as specified in the figure legends. For experiments conducted exclusively under normoxic conditions, cardiomyocytes were incubated for 3 h in identical environmental settings. In contrast, for experiments involving hypoxia, cells were incubated for 1 h under hypoxic conditions (BBL™ GasPak™, BD Biosciences) and then immediately collected for further analyses.

6.13. Induction of mitochondrial membrane permeabilization

Rat cardiomyocytes were loaded with 100 nmol/L tetramethylrhodamine-ethylester (TMRE) for 10 min, washed and maintained at 37°C in a control solution containing 140 nmol/L NaCl, 3.6 mM KCl, 1.2 mM $MgSO_4$, 1 mM $CaCl_2$, 20 mM HEPES, 5 mM glucose, at pH 7.4. To induce oxidative damage resulting in mPTP opening, TMRE-loaded cardiomyocytes were exposed to intermittent laser illumination at 560 nm (2s every 3s, 30 % laser intensity) using an Ar/Kr confocal system (Yokogawa CSU10, Nipkow spinning disk, Visitech, UK). Mitochondrial permeabilization was detected as a CsA-sensitive decrease in 590 nm fluorescence emission that progressed as a wave throughout the cell and eventually induced rigor contracture secondary to ATP depletion, as previously described [7]. Changes in fluorescent intensity were quantified with a commercial software (Voxcell Scan, Visitech, UK) and expressed as percentage of change throughout time with respect to the value obtained at baseline conditions. After loading with TMRE and prior to confocal laser illumination, cardiomyocytes were randomly assigned to different treatment groups as indicated in the figure legends ($n > 20$ cells per group from three to six different mice = 1 independent experiment).

6.14. ROS immuno-labelling and fluorescent microscopy

Hearts from the different experimental groups were removed from the Langendorff system and *in vivo* mice model, weighed and rapidly frozen in liquid nitrogen. *In situ* reactive oxygen species (ROS) were determined using labelling with dihydroethidium as described [35,104]. Tissue sections were examined by laser scanning confocal microscopy (Leica TCS SP2, Mannheim, Germany). A series of confocal optical sections were obtained using a Leica Planapo x40/1.00 or x63/1.32 objective lens. Each recorded image was obtained using dual-channel scanning and consisted of 1024×1024 pixels. To improve image quality and to obtain a high signal to noise ratio, each image from the series was signal-averaged. After data acquisition, the images were transferred to a workstation (Silicon Graphics, Fremont, CA) for restoration and three-dimensional reconstruction using Imaris 4.5 multichannel image processing software (Bitplane, Zurich, Switzerland). For each heart at least 10 random fields of vision were analysed with a fluorescent microscope (Leica-Microsystems) using a x40 Planapo objective. Immuno-labeled cryosections were studied using image analysis (Leica) and Image J software. Cardiomyocyte area and diameter were determined by delineating the β-actin-labeled myocytes. The fluorescence intensity was measured as AU/μm^2. For each quantification procedure a specific setting was established and kept constant in all measurements. Quantification of ROS was performed by measuring the fluorescence intensity using a range of 0–255 gray values. Arbitrary units of the fluorescence intensity were calculated per unit myocardial area (AU/μm^2).

6.15. RNA isolation and quantitative real time PCR analysis (qRT-PCR)

DNA-free total RNA was extracted from cardiomyocytes treated under different conditions and qRT-PCR was performed. The gene products for analysis of damage markers in cardiomyocytes were quantified using SYBR Green assays (Applied Biosystems). Results were expressed as fold-change compared to the control [105].The mRNA signal from hypoxanthine-guanine phosphoribosyl transferase *(hprt)* was used for normalization. Primers for the following genes were designed as described in references [35,40,60]: *hprt, prdx3* (peroxiredoxin 3), *sod* (superoxide dismutase), including *sod1* (cytoplasmic), *sod2* (mitochondrial), and *sod3* (extracellular), *iNos* (inducible nitric oxide synthase), and *mcp1* (monocyte chemoattractant protein-1). For each primer, 50 pmol of the sample was used.

CRediT authorship contribution statement

Hector A. Cabrera-Fuentes: Writing – review & editing, Writing – original draft, Visualization, Validation, Supervision, Project administration, Methodology, Investigation, Funding acquisition, Formal analysis, Conceptualization. **Marisol Ruiz-Meana:** Writing – review & editing, Supervision, Resources, Methodology, Investigation, Formal analysis. **Guillermo Barreto:** Writing – review & editing, Validation, Resources, Methodology, Investigation. **Victor L. Serebruany:** Writing – review & editing, Validation, Methodology, Formal analysis. **Jose T. Sánchez-Vega:** Writing – review & editing, Validation, Methodology, Formal analysis. **Eduardo Perez-Campos:** Writing – review & editing, Validation, Methodology, Formal analysis. **Sawa Kostin:** Writing – review & editing, Validation, Methodology, Data curation. **Andreas Böning:** Writing – review & editing, Visualization, Supervision, Methodology. **Efrén Emmanuel Jarquín González:** Writing – review & editing, Visualization, Validation, Methodology. **Ebtesam A. Al-Suhaimi:** Writing – review & editing, Validation, Formal analysis, Data curation. **Julian Rodriguez-Montesinos:** Writing – review & editing, Methodology, Investigation, Formal analysis. **Javier Inserte:** Writing – review & editing, Methodology, Investigation. **Sarah Pedretti:** Writing – review & editing, Methodology, Investigation. **Jonathan Yap:** Writing – review & editing, Methodology, Investigation. **Jason Irei:** Writing – review & editing, Methodology, Investigation. **Daniel G. Sedding:** Writing – review & editing, Validation, Supervision, Methodology, Investigation, Data curation. **Sandrine Lecour:** Writing – review & editing, Supervision, Methodology, Investigation. **Elisa A. Liehn:** Writing – review & editing, Visualization, Supervision, Methodology, Formal analysis. **David Garcia-Dorado:** Writing – review & editing, Writing – original draft, Validation, Supervision, Methodology, Investigation. **Derek J. Hausenloy:** Writing – review & editing, Writing – original draft, Supervision, Methodology, Investigation, Funding acquisition, Data curation. **William A. Boisvert:** Writing – review & editing, Writing – original draft, Visualization, Validation, Supervision, Project administration, Methodology, Investigation, Funding acquisition, Formal analysis, Conceptualization. **Klaus T. Preissner:** Writing – review & editing, Writing – original draft, Visualization, Validation, Supervision, Project administration, Methodology, Investigation, Funding acquisition, Formal analysis, Conceptualization.

Declaration of Competing Interest

The authors declare that they have no known competing financial interests or personal relationships, that could have appeared to influence the work reported in this paper.

Acknowledgments

We honor the memory and outstanding contributions of Dr. David Garcia-Dorado, whose pioneering work on myocardial I/R injury played a crucial role in the advancement of our knowledge in this field, and in the design and execution of groundbreaking studies, including his valued participation in the current study design. Dr. Garcia-Dorado's legacy will continue to inspire and guide future research in cardiovascular medicine. We thank Peter Volk, Maria Lucila Machado Suárez and Baerbel Fuehler for their excellent technical assistance. This work was supported in part by the German Research Foundation (DFG; Bonn, Germany) within the International Graduate School PROMISE (IRTG-1566, Giessen-Barcelona), the Excellence Cluster "Cardio-pulmonary System" (ECCPS, Giessen) and the Interdisciplinary Centre for Clinical Research (IZKF; Aachen, Germany). HACF is funded by a Start-up Grant of the ECCPS and the "Peter und Traudl Engelhorn-Foundation" (Weilheim, Germany), the Von Behring-Röntgen-Stiftung. (Marburg, Germany), the Singapore Heart Foundation (SHF/FG657P/2017) and part of the work was performed at the Department of Biochemistry, Medical School, Justus-Liebig-University, Giessen, Germany. DS is supported by the Excellence Cluster "REBIRTH" from the German Research Foundation (DFG, Bonn, Germany). SL is supported by the South African National Research Foundation and the University of Cape Town. EAL is supported Romanian Ministry of Education and Research (CNFIS-FDI-2024–0592). DH is supported by the Duke-NUS Signature Research Programme funded by the Ministry of Health, Singapore Ministry of Health's National Medical Research Council under its Singapore Translational Research Investigator Award (MOH-STaR21jun-0003), Centre Grant scheme (NMRC CG21APR1006), Collaborative Centre Grant scheme (NMRC/CG21APRC006), by the CArdiovascular DiseasE National Collaborative Enterprise (CADENCE) National Clinical Translational Program (MOH-001277–01), and the RIE2020/RIE2025 PREVENT-HF Industry Alignment Fund Pre-Positioning Programme (IAF-PP H23J2a0033), administered by A*STAR. MRM was funded by the Instituto de Salud Carlos III of the Spanish Ministry of Health through the projects FIS-PI22–00513, FIS-PI23-00068 and TACTICS (FORTALECE program), and co-founded by the European Union (FEDER) and by the Catalan Government (SGR-AGAUR). HACF and EEJG are members of the Comité Científico de Salud de los Servicios de Salud de Oaxaca (SSO), México.

Cytoprotective Role of RNase1

Our findings show that RNase1 administration significantly attenuates I/R injury by degrading extracellular RNA and thereby disrupting the eRNA–TACE–TNF-α signaling cascade. Treatment with RNase1 results in a marked reduction in infarct size and preserves cellular energy homeostasis during reperfusion. By neutralizing eRNA, RNase1 prevents downstream inflammatory signaling, positioning it as a promising therapeutic agent to limit myocardial damage and to preserve cardiac function following ischemic insult.

Comparative Efficacy and Synergism of RNase1 and CsA

Both RNase1 and CsA exhibit significant cardioprotective properties in our experimental models. However, the combination of RNase1 with CsA during reperfusion results in a more pronounced reduction in myocardial injurycompared to either agent alone. This synergistic effect likely arises from the dual targeting of distinct pathological pathways - eRNA-mediated inflammation and mitochondrial permeability transition pore opening - suggesting that combination therapy may offer an optimized strategy for clinical management of myocardial I/R injury.

Mechanistic and Translational Implications

This study provides novel mechanistic insights into the role of eRNA as an upstream trigger of TNF-α release via TACE activation in the context of myocardial I/R injury. Our results identify eRNA as a central mediator of sterile inflammation and cardiomyocyte death, contributing to the amplification of tissue damage. The data support the therapeutic targeting of extracellular nucleic acids using RNase1 as a strategy to disrupt this pathologic signaling loop. Future studies should focus on translating these findings into clinical contexts by determining optimal dosing regimens, evaluating long-term cardiac outcomes, and assessing the efficacy of RNase1 in large-animal and human models of myocardial infarction.

Data availability

Data will be made available on request.

References

[1] H.A. Cabrera-Fuentes, C. Alba-Alba, J. Aragones, J. Bernhagen, W.A. Boisvert, H. E. Botker, G. Cesarman-Maus, I. Fleming, D. Garcia-Dorado, S. Lecour, E. Liehn, M.S. Marber, N. Marina, M. Mayr, O. Perez-Mendez, T. Miura, M. Ruiz-Meana, E. M. Salinas-Estefanon, S.B. Ong, H.J. Schnittler, J.T. Sanchez-Vega, A. Sumoza-Toledo, C.W. Vogel, D. Yarullina, D.M. Yellon, K.T. Preissner, D.J. Hausenloy, Meeting report from the 2nd international symposium on new frontiers in cardiovascular research. Protecting the cardiovascular system from ischemia: between bench and bedside, Basic Res. Cardiol. 111 (1) (2016) 7.

[2] H.A. Cabrera-Fuentes, J. Aragones, J. Bernhagen, A. Boening, W.A. Boisvert, H. E. Botker, H. Bulluck, S. Cook, F. Di Lisa, F.B. Engel, B. Engelmann, F. Ferrazzi, P. Ferdinandy, A. Fong, I. Fleming, E. Gnaiger, S. Hernandez-Resendiz, S. B. Kalkhoran, M.H. Kim, S. Lecour, E.A. Liehn, M.S. Marber, M. Mayr, T. Miura, S. B. Ong, K. Peter, D. Sedding, M.K. Singh, M.S. Suleiman, H.J. Schnittler, R. Schulz, W. Shim, D. Tello, C.W. Vogel, M. Walker, Q.O. Li, D.M. Yellon, D. J. Hausenloy, K.T. Preissner, From basic mechanisms to clinical applications in heart protection, new players in cardiovascular diseases and cardiac theranostics: meeting report from the third international symposium on "new frontiers in cardiovascular research", Basic Res. Cardiol. 111 (6) (2016) 69.

[3] U. Landmesser, T. Thum, L. Tokgozoglu, T.J. Guzik, F. Cosentino, R. Hajjar, A. Goncalves, A. Laguna-Fernandez, P. Nioi, J.H. Prochaska, R. Rocha, S. Kathiresan, J. Marz, M.S. Maurer, C.J. O'Donnell, G. Passacquale, A. Tavridou, M. Van Heetvelde, A. Himmelmann, B. Meder, L. Roessig, F. Crea, T.F. Luscher, Pharmacotherapy of cardiovascular diseases from herbs and pills to nucleic acids, Eur. Heart J. (2025).

[4] D.M. Yellon, D.J. Hausenloy, Myocardial reperfusion injury, N. Engl. J. Med. 357 (11) (2007) 1121–1135.

[5] I. Andreadou, H.A. Cabrera-Fuentes, Y. Devaux, N.G. Frangogiannis, S. Frantz, T. Guzik, E.A. Liehn, C.P.C. Gomes, R. Schulz, D.J. Hausenloy, Immune cells as targets for cardioprotection: new players and novel therapeutic opportunities, Cardiovasc Res. 115 (7) (2019) 1117–1130.

[6] B.H. Zhao, A. Ruze, L. Zhao, Q.L. Li, J. Tang, N. Xiefukaiti, M.T. Gai, A.X. Deng, X. F. Shan, X.M. Gao, The role and mechanisms of microvascular damage in the ischemic myocardium, Cell Mol. Life Sci. 80 (11) (2023) 341.

[7] M. Ruiz-Meana, A. Abellan, E. Miro-Casas, D. Garcia-Dorado, Opening of mitochondrial permeability transition pore induces hypercontracture in Ca2+ overloaded cardiac myocytes, Basic Res. Cardiol. 102 (6) (2007) 542–552.

[8] F. Di Lisa, A. Carpi, V. Giorgio, P. Bernardi, The mitochondrial permeability transition pore and cyclophilin d in cardioprotection, Biochim. Biophys. Acta 1813 (7) (2011) 1316–1322.

[9] F. Di Lisa, N. Kaludercic, A. Carpi, R. Menabo, M. Giorgio, Mitochondria and vascular pathology, Pharmacol. Rep. 61 (1) (2009) 123–130.

[10] S.B. Ong, R.K. Dongworth, H.A. Cabrera-Fuentes, D.J. Hausenloy, Role of the MPTP in conditioning the heart - translatability and mechanism, Br. J. Pharmacol. 172 (8) (2015) 2074–2084.

[11] Y. Abdallah, C. Wolf, K. Meuter, H.M. Piper, H.P. Reusch, Y. Ladilov, Preconditioning with diazoxide prevents reoxygenation-induced rigor-type hypercontracture, J. Mol. Cell Cardiol. 48 (1) (2010) 270–276.

[12] Y. Ladilov, O. Efe, C. Schafer, B. Rother, S. Kasseckert, Y. Abdallah, K. Meuter, K. Dieter Schluter, H.M. Piper, Reoxygenation-induced rigor-type contracture, J. Mol. Cell Cardiol. 35 (12) (2003) 1481–1490.

[13] Y. Feng, X. Bao, J. Zhao, L. Kang, X. Sun, B. Xu, MSC-Derived exosomes mitigate myocardial Ischemia/Reperfusion injury by reducing neutrophil infiltration and the formation of neutrophil extracellular traps, Int. J. Nanomed. 19 (2024) 2071–2090.

[14] D. Garcia-Dorado, M. Ruiz-Meana, J. Inserte, A. Rodriguez-Sinovas, H.M. Piper, Calcium-mediated cell death during myocardial reperfusion, Cardiovasc. Res. 94 (2) (2012) 168–180.

[15] Y. Li, Y. Gao, G. Li, Preclinical multi-target strategies for myocardial ischemia-reperfusion injury, Front. Cardiovasc. Med. 9 (2022) 967115.

[16] D. Garcia-Dorado, P. Theroux, J.M. Duran, J. Solares, J. Alonso, E. Sanz, R. Munoz, J. Elizaga, J. Botas, F. Fernandez-Aviles, et al., Selective inhibition of the contractile apparatus. A new approach to modification of infarct size, infarct composition, and infarct geometry during coronary artery occlusion and reperfusion, Circulation 85 (3) (1992) 1160–1174.

[17] C. Schafer, Y. Ladilov, J. Inserte, M. Schafer, S. Haffner, D. Garcia-Dorado, H. M. Piper, Role of the reverse mode of the Na+/Ca2+ exchanger in reoxygenation-induced cardiomyocyte injury, Cardiovasc. Res. 51 (2) (2001) 241–250.
[18] M. Ruiz-Meana, D. Garcia-Dorado, M. Julia, J. Inserte, B. Siegmund, Y. Ladilov, M. Piper, F.P. Tritto, M.A. Gonzalez, J. Soler-Soler, Protective effect of HOE642, a selective blocker of Na+-H+ exchange, against the development of rigor contracture in rat ventricular myocytes, Exp. Physiol. 85 (1) (2000) 17–25.
[19] H.A. Prag, D. Aksentijevic, A. Dannhorn, A.V. Giles, J.F. Mulvey, O. Sauchanka, L. Du, G. Bates, J. Reinhold, D. Kula-Alwar, Z. Xu, L. Pellerin, R.J.A. Goodwin, M. P. Murphy, T. Krieg, Ischemia-Selective cardioprotection by malonate for Ischemia/Reperfusion injury, Circ. Res. 131 (6) (2022) 528–541.
[20] J. Abe, A. Vujic, H.A. Prag, M.P. Murphy, T. Krieg, Malonate given at reperfusion prevents post-myocardial infarction heart failure by decreasing ischemia/reperfusion injury, Basic Res. Cardiol. 119 (4) (2024) 691–697.
[21] L. Agullo, D. Garcia-Dorado, N. Escalona, M. Ruiz-Meana, M. Mirabet, J. Inserte, J. Soler-Soler, Membrane association of nitric oxide-sensitive guanylyl cyclase in cardiomyocytes, Cardiovasc. Res. 68 (1) (2005) 65–74.
[22] E.H. Mace, M.J. Kimlinger, F.Tt Billings, M.G. Lopez, Targeting soluble guanylyl cyclase during ischemia and reperfusion, Cells 12 (14) (2023).
[23] K.T. Preissner, W.A. Boisvert, D.J. Hausenloy, Surfing on the cardiovascular frontier wave, Thromb. Haemost. 113 (3) (2015) 439–440.
[24] D.J. Hausenloy, J.A. Barrabes, H.E. Botker, S.M. Davidson, F. Di Lisa, J. Downey, T. Engstrom, P. Ferdinandy, H.A. Carbrera-Fuentes, G. Heusch, B. Ibanez, E. K. Iliodromitis, J. Inserte, R. Jennings, N. Kalia, R. Kharbanda, S. Lecour, M. Marber, T. Miura, M. Ovize, M.A. Perez-Pinzon, H.M. Piper, K. Przyklenk, M. R. Schmidt, A. Redington, M. Ruiz-Meana, G. Vilahur, J. Vinten-Johansen, D. M. Yellon, D. Garcia-Dorado, Ischaemic conditioning and targeting reperfusion injury: a 30 year voyage of discovery, Basic Res. Cardiol. 111 (6) (2016) 70.
[25] S.B. Ong, S. Hernandez-Resendiz, G.E. Crespo-Avilan, R.T. Mukhametshina, X. Y. Kwek, H.A. Cabrera-Fuentes, D.J. Hausenloy, Inflammation following acute myocardial infarction: multiple players, dynamic roles, and novel therapeutic opportunities, Pharmacol. Ther. 186 (2018) 73–87.
[26] A. Boning, L. Flicker, J. Rodriguez-Montesinos, H. Cabrera-Fuentes, K. T. Preissner, B. Niemann, Z.T. Taghiyev, Remote ischemic preconditioning in patients undergoing cardiac surgery with six ischemic cycles, Perfusion 38 (7) (2023) 1418–1427.
[27] E.S. Santos, V.T. Baltar, M.P. Pereira, L. Minuzzo, A. Timerman, A. Avezum, Comparison between cardiac troponin I and CK-MB mass in acute coronary syndrome without st elevation, Arq. Bras. Cardiol. 96 (3) (2011) 179–187.
[28] W. Zhang, J. Zhang, Z. Wang, T. Li, L. Changyun, X. Kang, X. Cui, J. Yang, H. Qu, J. Duanmu, Y. Peng, K. Wang, L. Jin, P. Xie, W. Zheng, H. Shang, Y. Liu, Z. Tian, Z. Liu, Y. Jin, Y. Li, N. Li, X. Zhuo, Y. Wu, X. Shi, R. Ma, Y. Sun, K. Zhang, X. Fang, X. Hu, E. Dong, S. Zhang, Y. Zhang, Extracellular RIPK3 acts as a danger-associated molecular pattern to exaggerate cardiac Ischemia/Reperfusion injury, Circulation (2024).
[29] E.S. McErlean, S.A. Deluca, F. van Lente, Ft Peacock, J.S. Rao, C.A. Balog, S. E. Nissen, Comparison of troponin t versus creatine kinase-MB in suspected acute coronary syndromes, Am. J. Cardiol. 85 (4) (2000) 421–426.
[30] T. Artner, S. Sharma, I.M. Lang, Nucleic acid liquid biopsies in cardiovascular disease: Cell-free DNA liquid biopsies in cardiovascular disease, Atherosclerosis (2024) 118583.
[31] J. Winter, I. Klumpe, J. Heger, U. Rauch, H.P. Schultheiss, U. Landmesser, A. Dorner, Adenine nucleotide translocase 1 overexpression protects cardiomyocytes against hypoxia via increased ERK1/2 and AKT activation, Cell Signal 28 (1) (2016) 152–159.
[32] O. Ilinskaya, D.J. Hausenloy, H.A. Cabrera-Fuentes, M. Zenkova, Editorial: new advances in RNA targeting, Front. Pharmacol. 11 (2020) 468.
[33] S. Sharma, T. Artner, K.T. Preissner, I.M. Lang, Nucleic acid liquid biopsies in cardiovascular disease: Cell-free RNA liquid biopsies in cardiovascular disease, Atherosclerosis (2024) 118584.
[34] H.A. Cabrera-Fuentes, B. Niemann, P. Grieshaber, M. Wollbrueck, J. Gehron, K. T. Preissner, A. Boning, RNase1 as a potential mediator of remote ischaemic preconditioning for cardioprotectiondagger, Eur. J. Cardiothorac. Surg. 48 (5) (2015) 732–737.
[35] H.A. Cabrera-Fuentes, M. Ruiz-Meana, S. Simsekyilmaz, S. Kostin, J. Inserte, M. Saffarzadeh, S.P. Galuska, V. Vijayan, I. Barba, G. Barreto, S. Fischer, G. Lochnit, O.N. Ilinskaya, E. Baumgart-Vogt, A. Boning, S. Lecour, D. J. Hausenloy, E.A. Liehn, D. Garcia-Dorado, K.D. Schluter, K.T. Preissner, RNase1 prevents the damaging interplay between extracellular RNA and tumour necrosis factor-alpha in cardiac ischaemia/reperfusion injury, Thromb. Haemost. 112 (6) (2014) 1110–1119.
[36] S. Fischer, H.A. Cabrera-Fuentes, T. Noll, K.T. Preissner, Impact of extracellular RNA on endothelial barrier function, Cell Tissue Res. 355 (3) (2014) 635–645.
[37] E. Deindl, S. Fischer, K.T. Preissner, New directions in inflammation and immunity: the multi-functional role of the extracellular RNA/RNase system, Indian J. Biochem. Biophys. 46 (6) (2009) 461–466.
[38] S. Fischer, T. Gerriets, C. Wessels, M. Walberer, S. Kostin, E. Stolz, K. Zheleva, A. Hocke, S. Hippenstiel, K.T. Preissner, Extracellular RNA mediates endothelial-cell permeability via vascular endothelial growth factor, Blood 110 (7) (2007) 2457–2465.
[39] P. Stieger, J.M. Daniel, C. Tholen, J. Dutzmann, K. Knopp, D. Gunduz, M. Aslam, M. Kampschulte, A. Langheinrich, S. Fischer, H. Cabrera-Fuentes, Y. Wang, K. C. Wollert, J. Bauersachs, R. Braun-Dullaeus, K.T. Preissner, D.G. Sedding, Targeting of extracellular RNA reduces edema formation and infarct size and improves survival after myocardial infarction in mice, J. Am. Heart Assoc. 6 (6) (2017).
[40] H.A. Cabrera-Fuentes, M.L. Lopez, S. McCurdy, S. Fischer, S. Meiler, Y. Baumer, S. P. Galuska, K.T. Preissner, W.A. Boisvert, Regulation of monocyte/macrophage polarisation by extracellular RNA, Thromb. Haemost. 113 (3) (2015) 473–481.
[41] S. Fischer, T. Grantzow, J.I. Pagel, M. Tschernatsch, M. Sperandio, K.T. Preissner, E. Deindl, Extracellular RNA promotes leukocyte recruitment in the vascular system by mobilising proinflammatory cytokines, Thromb. Haemost. 108 (4) (2012) 730–741.
[42] E.A. Liehn, Cabrera-Fuentes HA. Inflammation between defense and disease: impact on tissue repair and chronic sickness, Discov. (Craiova) 3 (1) (2015) e42.
[43] A. Zernecke, K.T. Preissner, Extracellular ribonucleic acids (RNA) enter the stage in cardiovascular disease, Circ. Res. 118 (3) (2016) 469–479.
[44] H.A. Cabrera-Fuentes, K.T. Preissner, Extracellular RNA in Iron-Induced Hepatic Injury: Beyond TLR3 Toward an Integrated Inflammatory Axis, Toxicol. Rep. (2025) 102126. ISSN 2214-7500.
[45] M. Chemaly, V. McGilligan, M. Gibson, M. Clauss, S. Watterson, H.D. Alexander, A.J. Bjourson, A. Peace, Role of tumour necrosis factor alpha converting enzyme (TACE/ADAM17) and associated proteins in coronary artery disease and cardiac events, Arch. Cardiovasc. Dis. 110 (12) (2017) 700–711.
[46] P.M. Vidal, E. Lemmens, A. Avila, T. Vangansewinkel, A. Chalaris, S. Rose-John, S. Hendrix, ADAM17 is a survival factor for microglial cells in vitro and in vivo after spinal cord injury in mice, Cell Death Dis. 4 (12) (2013) e954.
[47] D.J. Hausenloy, E.A. Boston-Griffiths, D.M. Yellon, Cyclosporin a and cardioprotection: from investigative tool to therapeutic agent, Br. J. Pharmacol. 165 (5) (2012) 1235–1245.
[48] A.P. Halestrap, Calcium, mitochondria and reperfusion injury: a pore way to die, Biochem. Soc. Trans. 34 (Pt 2) (2006) 232–237.
[49] D.J. Hausenloy, M.R. Duchen, D.M. Yellon, Inhibiting mitochondrial permeability transition pore opening at reperfusion protects against ischaemia-reperfusion injury, Cardiovasc. Res. 60 (3) (2003) 617–625.
[50] S. Javadov, M. Karmazyn, N. Escobales, Mitochondrial permeability transition pore opening as a promising therapeutic target in cardiac diseases, J. Pharmacol. Exp. Ther. 330 (3) (2009) 670–678.
[51] S. Fischer, S. Gesierich, B. Griemert, A. Schanzer, T. Acker, H.G. Augustin, A. K. Olsson, K.T. Preissner, Extracellular RNA liberates tumor necrosis factor-alpha to promote tumor cell trafficking and progression, Cancer Res. 73 (16) (2013) 5080–5089.
[52] J.D. Webster, D. Vucic, The balance of TNF mediated pathways regulates inflammatory cell death signaling in healthy and diseased tissues, Front. Cell Dev. Biol. 8 (2020) 365.
[53] S. Lecour, R.W. James, When are pro-inflammatory cytokines SAFE in heart failure? Eur. Heart J. 32 (6) (2011) 680–685.
[54] E.A. Liehn, A.M. Piccinini, R.R. Koenen, O. Soehnlein, T. Adage, R. Fatu, A. Curaj, A. Popescu, A. Zernecke, A.J. Kungl, C. Weber, A new monocyte chemotactic protein-1/chemokine CC motif ligand-2 competitor limiting neointima formation and myocardial ischemia/reperfusion injury in mice, J. Am. Coll. Cardiol. 56 (22) (2010) 1847–1857.
[55] A. Covinhes, L. Gallot, C. Barrere, A. Vincent, C. Sportouch, C. Piot, B. Lebleu, J. Nargeot, P. Boisguerin, S. Barrere-Lemaire, Anti-apoptotic peptide for long term cardioprotection in a mouse model of myocardial ischemia-reperfusion injury, Sci. Rep. 10 (1) (2020) 18116.
[56] C. Kannemeier, A. Shibamiya, F. Nakazawa, H. Trusheim, C. Ruppert, P. Markart, Y. Song, E. Tzima, E. Kennerknecht, M. Niepmann, M.L. von Bruehl, D. Sedding, S. Massberg, A. Gunther, B. Engelmann, K.T. Preissner, Extracellular RNA constitutes a natural procoagulant cofactor in blood coagulation, Proc. Natl. Acad. Sci. USA 104 (15) (2007) 6388–6393.
[57] S. Fischer, M. Nishio, S.C. Peters, M. Tschernatsch, M. Walberer, S. Weidemann, R. Heidenreich, P.O. Couraud, B.B. Weksler, I.A. Romero, T. Gerriets, K. T. Preissner, Signaling mechanism of extracellular RNA in endothelial cells, FASEB J. Off. Publ. Fed. Am. Soc. Exp. Biol. 23 (7) (2009) 2100–2109.
[58] S. Fischer, K.T. Preissner, Extracellular nucleic acids as novel alarm signals in the vascular system. Mediators of defence and disease, Hamostaseologie 33 (1) (2013) 37–42.
[59] S. Antoniak, U. Boltzen, A. Eisenreich, C. Stellbaum, W. Poller, H.P. Schultheiss, U. Rauch, Regulation of cardiomyocyte full-length tissue factor expression and microparticle release under inflammatory conditions in vitro, J. Thromb. Haemost. JTH 7 (5) (2009) 871–878.
[60] S. Simsekyilmaz, H.A. Cabrera-Fuentes, S. Meiler, S. Kostin, Y. Baumer, E. A. Liehn, C. Weber, W.A. Boisvert, K.T. Preissner, A. Zernecke, Role of extracellular RNA in atherosclerotic plaque formation in mice, Circulation 129 (5) (2014) 598–606.
[61] H.A. Cabrera-Fuentes, K.T. Preissner, Abstract 20396: induction of ischemia-reperfusion injury by extracellular RNA: a case for tumor necrosis factor (TNF-α)—shedding, Circulation 130 (2014) A20396.
[62] K. Grote, M. Nicolai, U. Schubert, B. Schieffer, C. Troidl, K.T. Preissner, S. Bauer, S. Fischer, Extracellular ribosomal RNA acts synergistically with Toll-like receptor 2 agonists to promote inflammation, Cells 11 (9) (2022).
[63] G. Heusch, Myocardial ischemia/reperfusion: translational pathophysiology of ischemic heart disease, Med 5 (1) (2024) 10–31.
[64] A.M. Nicolau, P.G. Silva, H.P.G. Mejia, J.F. Granada, G.L. Kaluza, D. Burkhoff, T. Abizaid, B. Pileggi, A.F.D. Freire, R.R. Godinho, C.M. Campos, F.S. de Brito Jr., A. Abizaid, P.H.C. Melo, Molecular mechanisms of microvascular obstruction and dysfunction in percutaneous coronary interventions: from pathophysiology to Therapeutics-A comprehensive review, Int. J. Mol. Sci. 26 (14) (2025).
[65] J. Hefler, B.A. Marfil-Garza, S. Campbell, D.H. Freed, A.M.J. Shapiro, Preclinical systematic review & meta-analysis of cyclosporine for the treatment of myocardial ischemia-reperfusion injury, Ann. Transl. Med. 10 (18) (2022) 954.

[66] T.T. Cung, O. Morel, G. Cayla, G. Rioufol, D. Garcia-Dorado, D. Angoulvant, E. Bonnefoy-Cudraz, P. Guerin, M. Elbaz, N. Delarche, P. Coste, G. Vanzetto, M. Metge, J.F. Aupetit, B. Jouve, P. Motreff, C. Tron, J.N. Labeque, P.G. Steg, Y. Cottin, G. Range, J. Clerc, M.J. Claeys, P. Coussement, F. Prunier, F. Moulin, O. Roth, L. Belle, P. Dubois, P. Barragan, M. Gilard, C. Piot, P. Colin, F. De Poli, M. C. Morice, O. Ider, J.L. Dubois-Rande, T. Unterseeh, H. Le Breton, T. Beard, D. Blanchard, G. Grollier, V. Malquarti, P. Staat, A. Sudre, E. Elmer, M.J. Hansson, C. Bergerot, I. Boussaha, C. Jossan, G. Derumeaux, N. Mewton, M. Ovize, Cyclosporine before PCI in patients with acute myocardial infarction, N. Engl. J. Med. 373 (11) (2015) 1021–1031.
[67] L. Monassier, E. Ayme-Dietrich, G. Aubertin-Kirch, A. Pathak, Targeting myocardial reperfusion injuries with cyclosporine in the CIRCUS trial - pharmacological reasons for failure, Fundam. Clin. Pharmacol. 30 (2) (2016) 191–193.
[68] Z. Kiernan, G. Labate, Q. Chen, E.J. Lesnefsky, M. Quader, Infarct size reduction with cyclosporine a in circulatory death rat hearts: reducing effective ischemia time with therapy during reperfusion, Circ. Heart Fail 17 (10) (2024) e011846.
[69] W. Parichatikanond, R. Duangrat, N. Nuamnaichati, S. Mangmool, Role of A(1) adenosine receptor in cardiovascular diseases: bridging molecular mechanisms with therapeutic opportunities, Exp. Mol. Pathol. 141 (2025) 104952.
[70] Y. Li, R. Ye, H. Dai, J. Lin, Y. Cheng, Y. Zhou, Y. Lu, Exploring TNFR1: from discovery to targeted therapy development, J. Transl. Med. 23 (1) (2025) 71.
[71] A. Moatti, J.L. Cohen, The TNF-alpha/TNFR2 pathway: targeting a brake to release the Anti-tumor immune response, Front. Cell Dev. Biol. 9 (2021) 725473.
[72] S. Yang, J. Wang, D.D. Brand, S.G. Zheng, Role of TNF-TNF receptor 2 signal in regulatory t cells and its therapeutic implications, Front. Immunol. 9 (2018) 784.
[73] J. Silvain, J.P. Collet, C. Nagaswami, F. Beygui, K.E. Edmondson, A. Bellemain-Appaix, G. Cayla, A. Pena, D. Brugier, O. Barthelemy, G. Montalescot, J. W. Weisel, Composition of coronary thrombus in acute myocardial infarction, J. Am. Coll. Cardiol. 57 (12) (2011) 1359–1367.
[74] X.J. Zhang, X. Liu, M. Hu, G.J. Zhao, D. Sun, X. Cheng, H. Xiang, Y.P. Huang, R. F. Tian, L.J. Shen, J.P. Ma, H.P. Wang, S. Tian, S. Gan, H. Xu, R. Liao, T. Zou, Y. X. Ji, P. Zhang, J. Cai, Z.V. Wang, G. Meng, Q. Xu, Y. Wang, X.L. Ma, P.P. Liu, Z. Huang, L. Zhu, Z.G. She, X. Zhang, L. Bai, H. Yang, Z. Lu, H. Li, Pharmacological inhibition of arachidonate 12-lipoxygenase ameliorates myocardial ischemia-reperfusion injury in multiple species, Cell Metab. 33 (10) (2021) 2059–2075, e2010.
[75] A. Blasco, A. Rosell, R. Castejon, M.J. Coronado, A. Royuela, E. Ramil, S. Elorza, C. Thalin, P. Martin, B. Angulo, B. Rascon, S. Garcia-Gomez, I. Zabala, J. Ortega, L. Silva, C. Bellas, Analysis of NETs (neutrophil extracellular traps) in coronary thrombus and peripheral blood of patients with ST-segment elevation myocardial infarction, Thromb. Res. 235 (2024) 18–21.
[76] X. Wang, R. Xie, D. Zhao, G. Wang, L. Zhang, W. Shi, Y. Chen, T. Mo, Y. Du, X. Tian, W. Wang, R. Cao, Y. Ma, Y. Wei, Y. Wang, Blocking the TRAIL-DR5 pathway reduces cardiac Ischemia-Reperfusion injury by decreasing neutrophil infiltration and neutrophil extracellular traps formation, Cardiovasc. Drugs Ther. (2024).
[77] P.R. Rich, L.A. Mischis, S. Purton, J.T. Wiskich, The sites of interaction of triphenyltetrazolium chloride with mitochondrial respiratory chains, FEMS Microbiol. Lett. 202 (2) (2001) 181–187.
[78] S. Hernandez-Resendiz, R. Vilskersts, D. Aluja, I. Andreadou, P. Bencsik, M. Dambrova, P. Efentakis, F. Gao, Z. Giricz, J. Inserte, R. Kelly-Laubscher, A. Kiss, T. Krieg, B.R. Kwak, S. Lecour, G. Lopaschuk, M. Maczewski, M. Waszkiewicz, M. Okninska, P. Pagliaro, B. Podesser, H.A. Prag, M. Ruiz-Meana, T. Szabados, C.J. Zuurbier, P. Ferdinandy, D.J. Hausenloy, IMproving preclinical assessment of cardioprotective therapies (IMPACT): a small animal acute myocardial infarction randomized-controlled multicenter study on the effect of ischemic preconditioning, Basic Res. Cardiol. 120 (2) (2025) 335–346.
[79] Q. Xiang, X. Yi, X.H. Zhu, X. Wei, D.S. Jiang, Regulated cell death in myocardial ischemia-reperfusion injury, Trends Endocrinol. Metab. 35 (3) (2024) 219–234.
[80] J. Kranrod, A. Konkel, R. Valencia, A.M. Darwesh, R. Fischer, W.H. Schunck, J. M. Seubert, Cardioprotective properties of OMT-28, a synthetic analog of omega-3 epoxyeicosanoids, J. Biol. Chem. 300 (6) (2024) 107372.
[81] S. Li, X. Li, F. Xie, Y. Bai, J. Ma, Melatonin reduces myocardial cell damage in myocardial ischemia/reperfusion rats by inhibiting NLRP3 activation, Cell Mol Biol (Noisylegrand) 69 (15) (2023) 259–264.
[82] Z. Li, Z. Zheng, X. Dai, SIRT5 induces autophagy and alleviates myocardial infarction via desuccinylation of TOM1, BMC Cardiovasc. Disord. 24 (1) (2024) 464.
[83] Y.Q. Tan, W. Zhang, Z.C. Xie, J. Li, H.W. Chen, CaMK II in cardiovascular diseases, especially CaMK II-delta: friends or enemies, Drug Des. Dev. Ther. 18 (2024) 3461–3476.
[84] A. Javed, P.C. Ravi, S. Bilal Delvi, I. Faraz Hussain, G.A. Acosta, W. Iqbal, V. Krishnamaneni, S. Alasaadi, S. Pradhan, R. Vashisht, S. Modi, The relationship between myocardial infarction and estrogen use: a literature review, Cureus 15 (9) (2023) e46134.
[85] D.J. Burge, J. Eisenman, K. Byrnes-Blake, P. Smolak, K. Lau, S.B. Cohen, A. J. Kivitz, R. Levin, R.W. Martin, Y. Sherrer, J.A. Posada, Safety, pharmacokinetics, and pharmacodynamics of RSLV-132, an RNase-Fc fusion protein in systemic lupus erythematosus: a randomized, double-blind, placebo-controlled study, Lupus 26 (8) (2017) 825–834.
[86] M. Oliva, M. Munoz-Aguirre, S. Kim-Hellmuth, V. Wucher, A.D.H. Gewirtz, D. J. Cotter, P. Parsana, S. Kasela, B. Balliu, A. Vinuela, S.E. Castel, P. Mohammadi, F. Aguet, Y. Zou, E.A. Khramtsova, A.D. Skol, D. Garrido-Martin, F. Reverter, A. Brown, P. Evans, E.R. Gamazon, A. Payne, R. Bonazzola, A.N. Barbeira, A. R. Hamel, A. Martinez-Perez, J.M. Soria, G.T. Consortium, B.L. Pierce, M. Stephens, E. Eskin, E.T. Dermitzakis, A.V. Segre, H.K. Im, B.E. Engelhardt, K. G. Ardlie, S.B. Montgomery, A.J. Battle, T. Lappalainen, R. Guigo, B.E. Stranger, The impact of sex on gene expression across human tissues, Science 369 (6509) (2020).
[87] W. Bouma, M. Noma, S. Kanemoto, M. Matsubara, B.G. Leshnower, R. Hinmon, J. H. Gorman, 3rd, R.C. Gorman, Sex-related resistance to myocardial ischemia-reperfusion injury is associated with high constitutive ARC expression, Am. J. Physiol. Heart Circ. Physiol. 298 (5) (2010) H1510–H1517.
[88] S.A. Fortino, M. Wageh, R. Pontello, C. McGlory, D. Kumbhare, S.M. Phillips, G. Parise, Sex-Based differences in the myogenic response and inflammatory gene expression following eccentric contractions in humans, Front. Physiol. 13 (2022) 880625.
[89] Z. Wang, G. Zhang, S. Hu, M. Fu, P. Zhang, K. Zhang, L. Hao, S. Chen, Research progress on the protective effect of hormones and hormone drugs in myocardial ischemia-reperfusion injury, Biomed. Pharm. 176 (2024) 116764.
[90] A. Kher, M. Wang, B.M. Tsai, J.M. Pitcher, E.S. Greenbaum, R.D. Nagy, K. M. Patel, G.M. Wairiuko, T.A. Markel, D.R. Meldrum, Sex differences in the myocardial inflammatory response to acute injury, Shock 23 (1) (2005) 1–10.
[91] I. Martinez de Toda, M. Gonzalez-Sanchez, E. Diaz-Del Cerro, G. Valera, J. Carracedo, N. Guerra-Perez, Sex differences in markers of oxidation and inflammation. Implications for ageing, Mech. Ageing Dev. 211 (2023) 111797.
[92] A. Ruigomez, E.L. Masso-Gonzalez, S. Johansson, M.A. Wallander, L.A. Garcia-Rodriguez, Chest pain without established ischaemic heart disease in primary care patients: associated comorbidities and mortality, Br. J. Gen. Pract. 59 (560) (2009) e78–e86.
[93] L.M. Brewster, J. Fernand, Creatine kinase during non-ST-segment elevation acute coronary syndromes is associated with major bleeding, Open Heart 7 (2) (2020).
[94] N. Percie du Sert, V. Hurst, A. Ahluwalia, S. Alam, M.T. Avey, M. Baker, W. J. Browne, A. Clark, I.C. Cuthill, U. Dirnagl, M. Emerson, P. Garner, S.T. Holgate, D.W. Howells, N.A. Karp, S.E. Lazic, K. Lidster, C.J. MacCallum, M. Macleod, E. J. Pearl, O.H. Petersen, F. Rawle, P. Reynolds, K. Rooney, E.S. Sena, S. D. Silberberg, T. Steckler, H. Wurbel, The ARRIVE guidelines 2.0: updated guidelines for reporting animal research, BMC Vet. Res. 16 (1) (2020) 242.
[95] A. Curaj, S. Simsekyilmaz, M. Staudt, E. Liehn, Minimal invasive surgical procedure of inducing myocardial infarction in mice, J. Vis. Exp. (99) (2015) e52197.
[96] S.Y. Lim, S.M. Davidson, D.J. Hausenloy, D.M. Yellon, Preconditioning and postconditioning: the essential role of the mitochondrial permeability transition pore, Cardiovasc. Res. 75 (3) (2007) 530–535.
[97] C. Grohe, M. van Eickels, S. Wenzel, R. Meyer, H. Degenhardt, P.A. Doevendans, M.P. Heinemann, G. Ross, K.D. Schluter, Sex-specific differences in ventricular expression and function of parathyroid hormone-related peptide, Cardiovasc. Res. 61 (2) (2004) 307–316.
[98] S.Y. Lim, S.M. Davidson, A.J. Paramanathan, C.C. Smith, D.M. Yellon, D. J. Hausenloy, The novel adipocytokine visfatin exerts direct cardioprotective effects, J. Cell Mol. Med. 12 (4) (2008) 1395–1403.
[99] B. Liu, A. Li, Y. Qin, X. Tian, M. Gao, W. Jiang, G. Gong, Comparative study on isolation and mitochondrial function of adult mouse and rat cardiomyocytes, J. Mol. Cell Cardiol. 136 (2019) 64–71.
[100] M. Saffarzadeh, H.A. Cabrera-Fuentes, F. Veit, D. Jiang, K. Scharffetter-Kochanek, C.G. Gille, S.H.M. Rooijakkers, D. Hartl, K.T. Preissner, Characterization of rapid neutrophil extracellular trap formation and its cooperation with phagocytosis in human neutrophils, Discov. (Craiova) 2 (2) (2014) e19.
[101] J. Inserte, I. Barba, V. Hernando, D. Garcia-Dorado, Delayed recovery of intracellular acidosis during reperfusion prevents calpain activation and determines protection in postconditioned myocardium, Cardiovasc. Res. 81 (1) (2009) 116–122.
[102] M. Saffarzadeh, C. Juenemann, M.A. Queisser, G. Lochnit, G. Barreto, S. P. Galuska, J. Lohmeyer, K.T. Preissner, Neutrophil extracellular traps directly induce epithelial and endothelial cell death: a predominant role of histones, PLoS One 7 (2) (2012) e32366.
[103] N.W. Yang, J.M. Kim, G.J. Choi, S.J. Jang, Development and evaluation of the quick anaero-system-a new disposable anaerobic culture system, Korean J. Lab Med. 30 (2) (2010) 133–137.
[104] Z.A. Abassi, Y.D. Barac, S. Kostin, A. Roguin, E. Ovcharenko, H. Awad, A. Blank, O. Bar-Am, T. Amit, J. Schaper, M. Youdim, O. Binah, TVP1022 attenuates cardiac remodeling and kidney dysfunction in experimental volume overload-induced congestive heart failure, Circ. Heart Fail 4 (4) (2011) 463–473.
[105] S. De Rosa, F. Eposito, C. Carella, A. Strangio, G. Ammirati, J. Sabatino, F. G. Abbate, C. Iaconetti, V. Liguori, V. Pergola, A. Polimeni, S. Coletta, C. Gareri, B. Trimarco, G. Stabile, A. Curcio, C. Indolfi, A. Rapacciuolo, Transcoronary concentration gradients of circulating microRNAs in heart failure, Eur. J. Heart Fail 20 (6) (2018) 1000–1010.